

From Particle Currents to Tracer Diffusion: Universal Correlation Profiles in Single-File Dynamics

Aurélien Grabsch,¹ Théotim Berlioz,¹ Pierre Rizkallah,² Pierre Illien,² and Olivier Bénichou¹

¹*Sorbonne Université, CNRS, Laboratoire de Physique Théorique de la Matière Condensée (LPTMC), 4 Place Jussieu, 75005 Paris, France*

²*Sorbonne Université, CNRS, Physico-Chimie des Électrolytes et Nanosystèmes Interfaciaux (PHENIX), 4 Place Jussieu, 75005 Paris, France*

Single-file transport refers to the motion of particles in a narrow channel, such that they cannot bypass each other. This constraint leads to strong correlations between the particles, described by correlation profiles, which measure the correlation between a generic observable and the density of particles at a given position and time. They have recently been shown to play a central role in single-file systems. Up to now, these correlations have only been determined for diffusive systems in the hydrodynamic limit. Here, we consider a model of reflecting point particles on the infinite line, with a general individual stochastic dynamics. We show that the correlation profiles take a simple universal form, at arbitrary time. We illustrate our approach by the study of the integrated current of particles through the origin, and apply our results to representative models such as Brownian particles, run-and-tumble particles and Lévy flights. We further emphasise the generality of our results by showing that they also apply beyond the 1d case, and to other observables.

Introduction.— Single-file transport, where particles move in narrow channels with the constraint that they cannot bypass each other, has become a fundamental model for transport in confined systems [1–5]. Experimentally, this situation has been observed in various physical, chemical or biological systems, such as zeolites, colloidal suspensions, or carbon nanotubes [3–6]. Theoretically, it is a central field of statistical physics, relevant both at equilibrium and out-of-equilibrium [7, 8]. In this context, two key observables have received a notable attention: (i) the integrated current through the origin Q_t (defined as the number of particles which have crossed the origin from left to right, minus those from right to left, up to time t) [9–15]; (ii) the position X_t of a tracer [1, 2, 16–26], which can be monitored experimentally at various scales [3–5].

Because the order of the particles is conserved at all times, strong correlations between these observables and the density of particles $\rho(x, t)$ emerge. For instance, an increase of Q_t imposes a density at the right of the origin higher than average, and a lower on the left. A similar effect occurs with X_t : a large displacement of the tracer in a given direction involves the displacement of more and more particles in the same direction. This leads to a striking subdiffusive behaviour $\langle X_t^2 \rangle \propto \sqrt{t}$ [16] in contrast with the regular diffusion $\langle X_t^2 \rangle \propto t$.

Despite their importance, the quantification of the coupling between Q_t or X_t and $\rho(x, t)$ remains a broadly open question. Recently, they have been characterised for the Symmetric Exclusion Process, and other paradigmatic models of single-file diffusion [24–26]. In addition to their clear physical relevance, these correlations have also acquired a technical importance since they have been shown to satisfy a closed equation for these systems [24–26][27]. However, these results are limited to (i) the case of diffusive systems (in which the individual particles

have a diffusive motion); (ii) the long time behaviour; (iii) the specific case of X_t and Q_t .

Here, by considering a model of reflecting point particles on the infinite line, with an arbitrary individual stochastic dynamics, we overcome these limitations. We show that the correlation profiles take a simple universal form (with respect to the individual motion of the particles), at arbitrary time, and for a large class of observables (as defined below).

More precisely, we illustrate our approach by the study of the integrated current of particles through the origin, and apply our results to representative processes which go beyond Brownian particles, such as (i) run-and-tumble particles which are a key model to describe active transport [28, 29]; and (ii) Lévy flights which is an emblematic model of superdiffusion [30]. We further emphasise the generality of our results by showing that they also apply beyond the 1d case, and to other observables.

Model.— We first consider N particles on the real line, with position $\{x_i(t)\}_{i=1, \dots, N}$ at time t . In a second step, we will take the thermodynamic limit $N \rightarrow \infty$. Initially, the N particles are independently picked from a density $\rho_0(x)$, normalised such that $\int \rho_0(x) dx = N$. Each particle has a stochastic dynamics in time, described by its propagator $G_t(x|y)$, i.e. the prob. to find the particle at position x at time t , knowing that it was at position y at time 0. When this dynamics leads to a crossing between two particles, they are simply exchanged, leading to a reflection of the particles. This dynamics can be mapped onto the one of *noninteracting* particles (see Fig 1). While this formally applies to any propagator, this is especially relevant for Markovian dynamics, since the definition of the contact is more tricky in the non-Markovian case. The time evolution of the particles being independent from their initial distribution, we define two different types of averaging: (i) the average over the

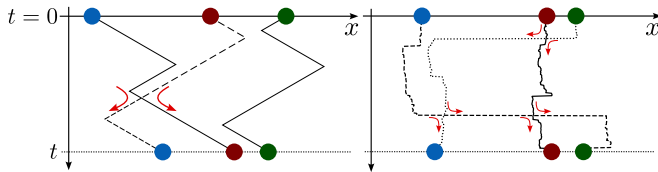


FIG. 1. The motion of reflective particles (illustrated by the arrows) can be mapped onto the motion of noninteracting particles (solid and dashed lines). Left: illustration with run-and-tumble particles, which move at a constant speed, and flip their direction at random times. When two particles collide, they flip their direction. Right: Lévy flights. When a particle collides another, it stops and the next particle is pushed. This can lead to a series of collisions.

time evolution of the particles, denoted for any function f ,

$$\langle f(\{x_i(t)\}) \rangle = \int \prod_{i=1}^N dx_n K_t(\{x_i\}|\{x_i(0)\}) f(\{x_i\}), \quad (1)$$

with K_t the N -particles propagator, and (ii) the average over the initial positions,

$$\overline{f(\{x_i(0)\})} = \int \prod_{n=1}^N dy_n \frac{\rho_0(y_n)}{N} f(\{y_i\}). \quad (2)$$

Although our approach can be applied to many observables, we will focus for concreteness on the integrated current through the origin, which measures the variation of the number of particles on the positive axis,

$$Q_t = \sum_i [\Theta(x_i(t)) - \Theta(x_i(0))], \quad (3)$$

where Θ is the Heaviside step function. We are interested in the statistical properties of this observable, and its correlations with the global density of particles

$$\rho(x, t) = \sum_i \delta(x - x_i(t)). \quad (4)$$

These two quantities are indeed expected to be strongly correlated. These correlations are encoded in the joint cumulant generating function $\ln \langle e^{\lambda Q_t + \chi \rho(x, t)} \rangle$, where λ and χ are the parameters of the generating function. We have used here the *annealed* averaging, as usually defined in statistical mechanics, which corresponds to averaging over both the time evolution and all the initial positions. For simplicity, we will focus on the lowest orders in χ , which are the cumulant generating function of the integrated current, $\psi_A(\lambda, t) \equiv \lim_{N \rightarrow \infty} \ln \langle e^{\lambda Q_t} \rangle$, and the correlation profile [24]

$$w_A(x, \lambda, t) \equiv \lim_{N \rightarrow \infty} \frac{\overline{\langle \rho(x, t) e^{\lambda Q_t} \rangle}}{\langle e^{\lambda Q_t} \rangle}. \quad (5)$$

These correlation profiles have been shown to play an important role, since they verify simple closed equations for several important models of single-file systems [24–26].

We also consider the case of a *quenched* initial condition, which corresponds to averaging over the time evolution of the typical initial positions of the particles. The initial condition is well-known to play a key role in single-file systems, as exemplified by “everlasting” effects on various observables [19, 20, 31–33]. In this case, the joint cumulant generating function is $\ln \langle e^{\lambda Q_t + \chi \rho(x, t)} \rangle$. At lowest orders in χ , this gives the quenched cumulant generating function $\psi_Q(\lambda, t) \equiv \lim_{N \rightarrow \infty} \ln \langle e^{\lambda Q_t} \rangle$, and the quenched correlation profile

$$w_Q(x, \lambda, t) \equiv \lim_{N \rightarrow \infty} \frac{\langle \rho(x, t) e^{\lambda Q_t} \rangle}{\langle e^{\lambda Q_t} \rangle}. \quad (6)$$

Results.— The key ingredient is the joint propagator of the N particles, which takes the form [34]

$$K_t(\vec{x}|\vec{y}) = \frac{1}{N!} \sum_{\sigma} \prod_{i=1}^N G_t(x_i|y_{\sigma(i)}), \quad (7)$$

where the sum runs over all permutations σ of the N particles. Computing first the averages (1,2), and then taking the thermodynamic limit $N \rightarrow \infty$ [35], we obtain that the cumulant generating function and the correlation profiles take a simple universal form (see Supplementary Material (SM) [36] for details of the derivation). In the annealed case,

$$\psi_A(\lambda, t) = \int dy \rho_0(y) \int (\tilde{G}_t^{(\lambda)}(x|y) - G_t(x|y)) dx, \quad (8)$$

$$w_A(x, \lambda, t) = \int \rho_0(y) \tilde{G}_t^{(\lambda)}(x|y) dy, \quad (9)$$

where we have defined the tilted propagator

$$\tilde{G}_t^{(\lambda)}(x|y) = e^{\lambda \Theta(x)} G_t(x|y) e^{-\lambda \Theta(y)}. \quad (10)$$

Similarly, in the quenched case,

$$\psi_Q(\lambda, t) = \int dy \rho_0(y) \ln \left[\int_{-\infty}^{\infty} \tilde{G}_t^{(\lambda)}(x|y) dx \right], \quad (11)$$

$$w_Q(x, \lambda, t) = \int dy \rho_0(y) \frac{\tilde{G}_t^{(\lambda)}(x|y)}{\int_{-\infty}^{\infty} \tilde{G}_t^{(\lambda)}(z|y) dz}. \quad (12)$$

These expressions hold for any propagator G_t of an individual particle, for any initial density of particles ρ_0 , and at arbitrary time t . They constitute the main results of this article. Note that our results hold in presence of external forces (a situation studied for instance in [37]) [38]. The key point of our derivation is that all the particles have the same dynamics (with the requirement that the

memory of the past is lost upon collision), and feel the presence of the other particles only when a collision occurs. The only ingredient needed is the one particle propagator G_t , either analytically or numerically [39]. We now give the example of run-and-tumble particles, for which the propagator is known explicitly. This will allow us to discuss on a concrete example the physics of these correlation profiles. Formulas for the cases of Brownian particles and Lévy flights are given in SM [36].

Application: run-and-tumble particles.— We consider a system of run-and-tumble particles, which is an important model of active particles, involved in various contexts [28, 29]. These particles move at constant speed v_0 , and flip their direction of motion with rate γ . When two particles collide, they are reflected (see Fig. 1). For simplicity, we will consider a step initial density of particles $\rho_0(x) = \rho_+ \Theta(x) + \rho_- \Theta(-x)$. The Laplace transform of the propagator of an individual particle takes a simple form [28]. We can easily obtain the annealed profile and cumulant generating function in the Laplace domain since the expressions (8,9) are linear in the propagator. The inverse Laplace transform can be computed explicitly using the expressions given in [12], and we get $\psi_A(\lambda, t) = \frac{\omega}{2} v_0 t e^{-\gamma t} (\mathbf{I}_0(\gamma t) + \mathbf{I}_1(\gamma t))$, where we have denoted $\omega = \rho_+(e^{-\lambda} - 1) + \rho_-(e^\lambda - 1)$, by analogy with the single parameter identified in the simple exclusion process (SEP) [9], and \mathbf{I}_ν is a modified Bessel function. Similarly, the correlation profile reads

$$w_A(x > 0, \lambda, t) = \rho_+ + \frac{\rho_- e^\lambda - \rho_+}{2} \Theta(v_0 t - x) \times \left(e^{-\frac{\gamma x}{v_0}} + \frac{\gamma x}{v_0} \int_1^{\frac{v_0 t}{x}} \frac{e^{-\frac{\gamma x T}{v_0}} \mathbf{I}_1(\frac{\gamma x}{v_0} \sqrt{T^2 - 1})}{\sqrt{T^2 - 1}} dT \right). \quad (13)$$

This profile, represented in Fig. 2, quantifies the correlation between the observable Q_t and the density of particles $\rho(x, t)$. When $\lambda > 0$, $w_A(x > 0, \lambda, t) \geq \rho_+$, indicating that an increase of the current yields an increase of the density at the right of the origin. We emphasise that (i) our approach captures the full dynamics of the profile w_A (13), illustrated in Fig. 2. In particular it presents a sharp cutoff at $x = v_0 t$, which is a consequence of the finite speed v_0 of the particles, showing that Q_t and $\rho(x, t)$ are decorrelated for $x > v_0 t$; (ii) the dependence of the profile (13) in ρ_+ , ρ_- and λ is in fact a general feature which holds for any propagator G_t , and is only a consequence of the choice of the observable Q_t and the initial step of density $\rho_0(x)$.

We now demonstrate that our approach can be extended in several important directions (see SM [36] for details).

Extension: other geometry.— Our approach can be extended beyond the one dimensional case, in particular to any tree geometry. An important example which has generated lots of works is the comb lattice [40–42]. Comb

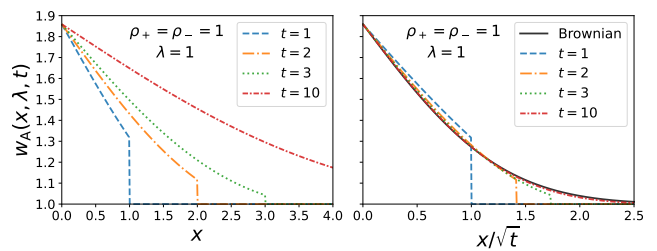


FIG. 2. Annealed correlation profile w_A (13) for run-and-tumble particles, with $v_0 = 1$ and $\gamma = 1$. Left: Profile as a function of x for different times. Right: Profile as a function of the rescaled variable x/\sqrt{t} at different times. For $t \rightarrow \infty$, it converges to the profile for diffusive particles (solid black lines), with a diffusion constant $D = v_0^2/(2\gamma) = \frac{1}{2}$.

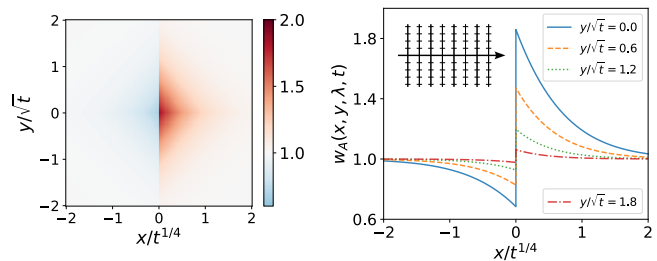


FIG. 3. Correlation profile $w_A(\vec{r} = (x, y), \lambda, t)$ for random walkers on a comb lattice in the annealed case (represented on the right plot), in the continuous limit. Left: 2D representation. The profile is a scaling function of $x/t^{1/4}$ and y/\sqrt{t} . Right: Profile as a function of x for fixed values of y .

structures have been developed to represent diffusion in critical percolation clusters, with the backbone and teeth of the comb mimicking the quasi-linear structure and the dead ends of percolation clusters [43]. More recently, the comb model has been used to account for transport in real systems such as spiny dendrites [44], diffusion of cold atoms [45] and diffusion in crowded media [46]. It is a two dimensional lattice in which all the links parallel to the x -axis have been removed, except those on the axis itself, called the backbone (see the inset in Fig. 3). The propagator of a particle performing a random walk on this lattice is given in [41]. In the continuous limit, the results (8,9,11,12) straightforwardly extend to this case, and leads to the correlation profile $w_A(\vec{r}, \lambda, t)$ shown in Fig. 3. It presents a different scaling with time in the two directions x and y , because particles can diffuse in the teeth of the comb, but horizontal motion is slowed down because it is only possible at $y = 0$.

Extension: other observables.—The above discussion can be extended to observables of the form

$$\mathcal{O}[f, g] = \sum_i [f(x_i(t)) - g(x_i(0))] , \quad (14)$$

where f and g are two given functions, with $f(x) \underset{x \rightarrow \pm\infty}{\simeq} g(x)$ to ensure convergence of the sum. The case of the

integrated current Q_t corresponds to $f = g = \Theta$. In general, the above results (8,9,11,12) still hold, but with the tilted propagator

$$\tilde{G}_t^{(\lambda)}(x|y) = e^{\lambda f(x)} G_t(x|y) e^{-\lambda g(y)}. \quad (15)$$

This provides in particular the profiles in the case of a generalised current $J_t(X)$, defined by $f(x) = \Theta(x - X)$ and $g(x) = \Theta(x)$. This observable measures the difference between the number of particles at the right of X at time t with the number of particles on the positive axis at $t = 0$. It has proved to be especially relevant since it can be used to find the position X_t of a tracer particle [47, 48], given by $J_t(X_t) = 0$, meaning that no particle can cross the tracer. However, this only provides the final position X_t , and not the displacement $X_t - X_0$ (X_0 being the position of the first particle to the right of the origin, which is random).

Extension: tracer particle.— Nevertheless, our method can be adapted to directly study the displacement of a tracer (placed initially at the origin for simplicity). So far, the only available studies concern the distribution of the tracer only [34, 49], and not its correlations with the other particles, which are our main focus here.

Extending the ideas of [1, 20, 34, 49, 50], the correlation profiles can be computed by noticing that the tracer can be mapped onto the "middle" particle of the system of noninteracting particles introduced above. We now consider a finite system of $2N + 1$ particles, with initially N particles on the negative axis (positions $x_{-n}(t)$), N particles on the positive axis (positions $x_n(t)$), and a tracer initially at the origin ($x_0(t)$). We define the average over the initial positions as

$$\overline{f(\{x_i(0)\})} = \int_{-\infty}^0 \prod_{n=1}^N \frac{\rho_0(y_{-n}) dy_{-n}}{N} \int_0^{\infty} \prod_{n=1}^N \frac{\rho_0(y_n) dy_n}{N} f(y_{-N}, \dots, y_{-1}, y_0 = 0, y_1, \dots, y_N). \quad (16)$$

The average over the time evolution is still given by (1). The probability of finding the tracer at position X at time t , with initially the particles at positions $\{x_i(0)\}$ can be obtained by imposing that there are still N particles to the left of the tracer, and N to the right,

$$P_t(X|\{x_i(0)\}) \equiv \langle \delta(X - x_0(t)) \rangle \propto \int_{-\infty}^X \prod_{n=1}^N dx_{-n} \int_X^{\infty} \prod_{n=1}^N dx_n K_t(\{x_n\}|_{x_0=X}|\{x_i(0)\}). \quad (17)$$

Using the expression of the joint propagator (7), and averaging over the time evolution and the initial positions (assumed to be annealed for simplicity), we obtain the distribution of $x_0(t)$ in the thermodynamic limit,

$$P_t(X) \equiv \lim_{N \rightarrow \infty} \overline{\langle \delta(X - x_0(t)) \rangle} = \int_{-\pi}^{\pi} f_t(X, \theta) e^{\phi_t(X, \theta)} d\theta, \quad (18)$$

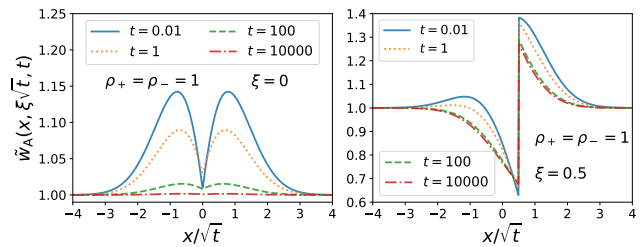


FIG. 4. Conditional density profiles \tilde{w}_A , for reflecting Brownian particles with diffusion coefficient $D = \frac{1}{2}$, with a tracer at position $X = \xi\sqrt{t}$, at different times t . Left: case $\xi = 0$, corresponding to a tracer conditioned to be at its mean position. Right: $\xi = 0.5$.

where the integration over θ enforces the noncrossing constraint. The functions f_t and ϕ_t are expressed in terms of the propagator G_t (assumed translationally invariant and symmetric), its integral $F_t(z) = \int_z^{\infty} G_t(x|0) dx$ and the initial density of particles ρ_0 . The exact expressions are given in SM [36]. The distribution (18) extends to the out-of-equilibrium case of an arbitrary initial density ρ_0 , such as a step initial condition, the result of [49] obtained in the equilibrium case of a constant density. Here, we obtain in addition the full spatial dependence of the correlations between the position of the tracer and the density of surrounding particles, which takes the following simple and universal form

$$\begin{aligned} \tilde{w}_A(x, X, t) &\equiv \lim_{N \rightarrow \infty} \frac{\overline{\langle \rho(x, t) \delta(X - x_0(t)) \rangle}}{\langle \delta(X - x_0(t)) \rangle} \\ &= \alpha_t^{\pm}(X) G_t(x|0) + \beta_t^{\pm}(X) \rho_{\mp} F_t(\pm x) + \rho_{\pm} F_t(\mp x), \end{aligned} \quad (19)$$

where the superscript \pm stands for $x \gtrless X$, with α_t^{\pm} and β_t^{\pm} given explicitly in SM [36]. We stress that the spatial dependence of these profiles are fully encoded in the propagator G_t (and its integral F_t). Note that we have considered in Eq. (19) here conditional profiles, which measure the mean density of particles conditioned on having observed the tracer at X at time t . In contrast, we have previously considered correlation profiles $\overline{\langle \rho(x, t) e^{\lambda x_0(t)} \rangle} / \langle e^{\lambda x_0(t)} \rangle$. The two formulations are equivalent in the limit $t \rightarrow \infty$ [25, 36], but not at arbitrary time. It turns out that the correlation profiles are more convenient to study observables of the form (14), while the conditional profiles are more suited to study tracer particles, since they take a simple form. These conditional profiles are shown in Fig. 4 for reflective Brownian particles. At long times, they reach their asymptotic values computed in [24], but at arbitrary times they have a more complex structure, mostly due to the presence of the tracer at the origin at $t = 0$ (first term in (19)).

Extension: two tracers.— Our approach can be extended to the important and largely unexplored situa-

tion of two tracers of positions $X_1(t)$ and $X_2(t)$. The only available studies in single-file systems concern the symmetric exclusion process and its limits [51–54], and the distance between two different particles at different times [55] which does not give access to the joint position of two tracers at the same time. We still obtain a simple form for the density profile conditioned on observing the first tracer at X and the second tracer at Y . As a byproduct, we obtain the strikingly simple, universal, and to the best of our knowledge new expression for the covariance of the displacements of two tracers,

$$\frac{\text{Cov}(X_1, X_2)}{\sqrt{\text{Var}(X_1)\text{Var}(X_2)}} \underset{t \rightarrow \infty}{\simeq} \frac{\int_z^\infty dx \int_x^\infty dy g(y)}{\int_0^\infty dx \int_x^\infty dy g(y)}, \quad (20)$$

where $z = [X_1(0) - X_2(0)]/\sigma_t$, and σ_t the long time scaling of the propagator $G_t(x|y) = g(\frac{x-y}{\sigma_t})/\sigma_t$.

Conclusion. — We have shown that the correlation profiles in single-file systems take the strikingly simple universal form (9-12). The approach is general and applies to: (i) a broad range of dynamics (including with external forces or non-Markovian dynamics provided that the memory is lost upon collision); (ii) arbitrary time (note that these results are not accessible via the classical Macroscopic Fluctuation Theory [56], which is limited to the large time behaviour of diffusive systems [57]); (iii) different initial conditions (annealed and quenched [58]); (iv) various observables (the form (14) includes the joint statistics of several currents [36]); (v) geometries not restricted to the single-file constraint (illustrated by the comb geometry). In addition, beyond the clear physical relevance of the correlation profiles, the simplicity of (9-12) further highlights their key role to describe transport properties in confined geometry [13–15, 18, 24–26, 47, 48, 59].

[1] D. G. Levitt, *Phys. Rev. A* **8**, 3050 (1973).
 [2] R. Arratia, *Ann. Probab.* **11**, 362 (1983).
 [3] K. Hahn, J. Kärger, and V. Kukla, *Phys. Rev. Lett.* **76**, 2762 (1996).
 [4] Q.-H. Wei, C. Bechinger, and P. Leiderer, *Science* **287**, 625 (2000).
 [5] B. Lin, M. Meron, B. Cui, S. A. Rice, and H. Diamant, *Phys. Rev. Lett.* **94**, 216001 (2005).
 [6] S. Cambré, B. Schoeters, S. Luyckx, E. Goovaerts, and W. Wenseleers, *Phys. Rev. Lett.* **104**, 207401 (2010).
 [7] P. L. Krapivsky, S. Redner, and E. Ben-Naim, *A kinetic view of statistical physics* (Cambridge University Press, 2010).
 [8] T. Chou, K. Mallick, and R. K. Zia, *Rep. Prog. Phys.* **74**, 116601 (2011).
 [9] B. Derrida and A. Gerschenfeld, *J. Stat. Phys.* **136**, 1 (2009).
 [10] B. Derrida and A. Gerschenfeld, *J. Stat. Phys.* **137**, 978 (2009).

[11] P. Krapivsky and B. Meerson, *Phys. Rev. E* **86**, 031106 (2012).
 [12] T. Banerjee, S. N. Majumdar, A. Rosso, and G. Schehr, *Phys. Rev. E* **101**, 052101 (2020).
 [13] K. Mallick, H. Moriya, and T. Sasamoto, *Phys. Rev. Lett.* **129**, 040601 (2022).
 [14] E. Bettelheim, N. R. Smith, and B. Meerson, *Phys. Rev. Lett.* **128**, 130602 (2022).
 [15] D. S. Dean, S. N. Majumdar, and G. Schehr, *arXiv:2303.08961* (2023).
 [16] T. E. Harris, *J. Appl. Probab.* **2**, 323 (1965).
 [17] A. Ryabov and P. Chvosta, *J. Chem. Phys.* **136**, 064114 (2012).
 [18] P. L. Krapivsky, K. Mallick, and T. Sadhu, *Phys. Rev. Lett.* **113**, 078101 (2014).
 [19] P. L. Krapivsky, K. Mallick, and T. Sadhu, *J. Stat. Mech: Theory Exp.* **2015**, P09007 (2015).
 [20] T. Sadhu and B. Derrida, *J. Stat. Mech: Theory Exp.* **2015**, P09008 (2015).
 [21] J. Cividini, A. Kundu, S. N. Majumdar, and D. Mukamel, *J. Stat. Mech: Theory Exp.* **2016**, 053212 (2016).
 [22] J. Cividini, A. Kundu, S. N. Majumdar, and D. Mukamel, *J. Phys. A* **49**, 085002 (2016).
 [23] A. Kundu and J. Cividini, *Europhys. Lett.* **115**, 54003 (2016).
 [24] A. Poncet, A. Grabsch, P. Illien, and O. Bénichou, *Phys. Rev. Lett.* **127**, 220601 (2021).
 [25] A. Grabsch, A. Poncet, P. Rizkallah, P. Illien, and O. Bénichou, *Sci. Adv.* **8**, eabm5043 (2022).
 [26] A. Grabsch, P. Rizkallah, A. Poncet, P. Illien, and O. Bénichou, *Phys. Rev. E* **107**, 044131 (2023).
 [27] Note that, since the publication of [25] in which this closed equation first appears, the exactness of the equation has been proved [13] using the inverse scattering method (see also [14, 59]).
 [28] G. H. Weiss, *Physica A* **311**, 381 (2002).
 [29] J. Tailleur and M. E. Cates, *Phys. Rev. Lett.* **100**, 218103 (2008).
 [30] J.-P. Bouchaud and A. Georges, *Phys. Rep.* **195**, 127 (1990).
 [31] N. Leibovich and E. Barkai, *Phys. Rev. E* **88**, 032107 (2013).
 [32] A. Poncet, O. Bénichou, and P. Illien, *Phys. Rev. E* **103**, L040103 (2021).
 [33] J. Krug, H. Kallabis, S. N. Majumdar, S. J. Cornell, A. J. Bray, and C. Sire, *Phys. Rev. E* **56**, 2702 (1997).
 [34] C. Rödenbeck, J. Kärger, and K. Hahn, *Phys. Rev. E* **57**, 4382 (1998).
 [35] We have introduced the initial density of particles ρ_0 with the constraint that it is normalised to N . In the thermodynamic limit $N \rightarrow \infty$, this constraint relaxes and one can consider non-normalised initial densities, such as $\rho_0(x) = \rho$ constant.
 [36] Supplementary Material.
 [37] A. P. Antonov, A. Ryabov, and P. Maass, *Phys. Rev. Lett.* **129**, 080601 (2022).
 [38] Note that our results hold in the presence of external forces, but not for arbitrary interparticle interactions, since this latter case involves the full many-body propagator which cannot be reduced to a single-particle propagator in the general case.
 [39] If the propagator is known analytically, our main results (8-12) yield explicit expressions for the cumulants and profiles. If the propagator is obtained numerically,

our results provide a straightforward way to compute these observables numerically by at most two numerical integrations.

- [40] O. Bénichou, P. Illien, G. Oshanin, A. Sarracino, and R. Voituriez, *Phys. Rev. Lett.* **115**, 220601 (2015).
- [41] P. Illien and O. Bénichou, *J. Phys. A Math. Theor.* **49**, 265001 (2016).
- [42] A. Iomin, V. Méndez, and W. Horsthemke, *Fractional dynamics in comb-like structures* (World Scientific, 2018).
- [43] G. H. Weiss and S. Havlin, *Physica A* **134**, 474 (1986).
- [44] V. Méndez and A. Iomin, *Chaos Solitons Fractals* **53**, 46 (2013).
- [45] Y. Sagi, M. Brook, I. Almog, and N. Davidson, *Phys. Rev. Lett.* **108**, 093002 (2012).
- [46] F. Höfling and T. Franosch, *Rep. Prog. Phys.* **76**, 046602 (2013).
- [47] T. Imamura, K. Mallick, and T. Sasamoto, *Phys. Rev. Lett.* **118**, 160601 (2017).
- [48] T. Imamura, K. Mallick, and T. Sasamoto, *Commun. Math. Phys.* **384**, 1409 (2021).
- [49] C. Hegde, S. Sabhapandit, and A. Dhar, *Phys. Rev. Lett.* **113**, 120601 (2014).
- [50] P. L. Krapivsky, K. Mallick, and T. Sadhu, *J. Stat. Phys.* **160**, 885 (2015).
- [51] S. Majumdar and M. Barma, *Physica A* **177**, 366 (1991).
- [52] O. Takeshi, S. Goto, T. Matsumoto, A. Nakahara, and M. Otsuki, *Phys. Rev. E* **88**, 062108 (2013).
- [53] T. Ooshida and M. Otsuki, *J. Phys. Condens. Matter* **30**, 374001 (2018).
- [54] A. Poncet, O. Bénichou, V. Démery, and G. Oshanin, *Phys. Rev. E* **97**, 062119 (2018).
- [55] S. Sabhapandit and A. Dhar, *J Stat. Mech.* **2015**, P07024 (2015).
- [56] L. Bertini, A. De Sole, D. Gabrielli, G. Jona-Lasinio, and C. Landim, *Rev. Mod. Phys.* **87**, 593 (2015).
- [57] For diffusive systems, the MFT gives access to correlation profiles of the form $\langle \rho(x, \tau T) e^{\lambda \mathcal{O}_T} \rangle / \langle e^{\lambda \mathcal{O}_T} \rangle$ with T large and $0 \leq \tau \leq 1$. Here, we have obtained correlation profiles of the form $\langle \rho(x, t) e^{\lambda \mathcal{O}_t} \rangle / \langle e^{\lambda \mathcal{O}_t} \rangle$ for arbitrary t .
- [58] The quenched case is notoriously more difficult than the annealed case: for instance while the annealed cumulant generating function of the current in the symmetric exclusion process has been determined in [9], its quenched counterpart is still missing.
- [59] A. Krajenbrink and P. Le Doussal, *Phys. Rev. E* **107**, 014137 (2023).

Supplementary Material for From Particle Currents to Tracer Diffusion: Universal Correlation Profiles in Single-File Dynamics

Aurélien Grabsch, Théotim Berlioz, Pierre Rizkallah, Pierre Illien, and Olivier Bénichou

CONTENTS

I. Annealed vs quenched correlation functions	7
II. Derivation of the cumulants and correlations	8
A. Average over the time evolution	8
B. Average over the initial positions in the annealed case	9
C. Average over the initial positions in the quenched case	10
D. Applications	11
1. Brownian particles	11
2. Run and tumble particles	11
3. Lévy flights	11
III. The comb geometry	12
A. Propagator in the continuous limit	12
B. Current through the bond $(0, 0) - (1, 0)$	13
IV. Derivation of the cumulants and correlations for the tracer	14
A. Averaging over the time evolution	14
B. Average over the initial positions	15
V. The case of two tracers	17
A. Averaging over the time evolution	17
B. Averaging over the initial condition	18
C. Long time limit: alternative derivation	20
VI. Conditional profiles vs correlation profiles	21
References	21

I. ANNEALED VS QUENCHED CORRELATION FUNCTIONS

We consider the general observable

$$\mathcal{O}_t[f, g] = \sum_i [f(x_i(t)) - g(x_i(0))] , \quad (\text{S1})$$

with $f(x) \underset{x \rightarrow \pm\infty}{\simeq} g(x)$ to ensure convergence in the limit $N \rightarrow \infty$. We also define the density of particles

$$\rho(x, t) = \sum_i \delta(x - x_i(t)) . \quad (\text{S2})$$

The joint statistical properties of these two observables are encoded in the joint cumulant generating functions. In the annealed case, it takes the form

$$\log \overline{\langle e^{\lambda \mathcal{O}_t + \chi \rho(x, t)} \rangle} = \log \overline{\langle e^{\lambda \mathcal{O}_t} \rangle} + \chi \frac{\overline{\langle \rho(x, t) e^{\lambda \mathcal{O}_t} \rangle}}{\overline{\langle e^{\lambda \mathcal{O}_t} \rangle}} + O(\chi^2) . \quad (\text{S3})$$

Similarly, we consider the quenched joint cumulant generating function

$$\overline{\log \langle e^{\lambda \mathcal{O}_t + \chi \rho(x,t)} \rangle} = \overline{\log \langle e^{\lambda \mathcal{O}_t} \rangle} + \chi \frac{\overline{\langle \rho(x,t) e^{\lambda \mathcal{O}_t} \rangle}}{\overline{\langle e^{\lambda \mathcal{O}_t} \rangle}} + O(\chi^2). \quad (\text{S4})$$

This motivates the definition of the correlation profiles w_A and w_Q in the main text.

II. DERIVATION OF THE CUMULANTS AND CORRELATIONS

A. Average over the time evolution

We begin by computing the moment generating function for a given number N of particles. We will denote $\{y_i = x_i(0)\}$ the positions of the particles at initial time, which are at the moment treated as parameters. By definition,

$$\begin{aligned} \langle e^{\lambda \mathcal{O}_t} \rangle &= \int_{-\infty}^{\infty} dx_1 \cdots dx_N K_t(\{x_i\}|\{y_i\}) \prod_{i=1}^N e^{\lambda(f(x_i) - g(y_i))} \\ &= \frac{1}{N!} \sum_{\sigma} \prod_{i=1}^N e^{-\lambda g(y_i)} \int_{-\infty}^{\infty} G_t(x|y_{\sigma(i)}) e^{\lambda f(x)} dx \\ &= \prod_{i=1}^N e^{-\lambda g(y_i)} \int_{-\infty}^{\infty} G_t(x|y_i) e^{\lambda f(x)} dx, \end{aligned} \quad (\text{S5})$$

since all the integrals are independent and equivalent. Similarly, we can compute

$$\begin{aligned} \langle \rho(x,t) e^{\lambda \mathcal{O}_t} \rangle &= \sum_n \int_{-\infty}^{\infty} dx_1 \cdots dx_N \delta(x - x_n) K_t(\{x_i\}|\{y_i\}) \prod_{i=1}^N e^{\lambda(f(x_i) - g(y_i))} \\ &= \frac{1}{N!} \sum_n \sum_{\sigma} G_t(x|y_{\sigma(n)}) e^{\lambda f(x) - \lambda g(y_n)} \prod_{i \neq n} e^{-\lambda g(y_i)} \int_{-\infty}^{\infty} G_t(x'|y_{\sigma(i)}) e^{\lambda f(x')} dx' \\ &= \frac{1}{N!} \sum_n \sum_q \sum_{\sigma, \sigma(n)=q} G_t(x|y_q) e^{\lambda f(x) - \lambda \sum_i g(y_i)} \prod_{j \neq q} \int_{-\infty}^{\infty} G_t(x'|y_j) e^{\lambda f(x')} dx' \\ &= \sum_q G_t(x|y_q) e^{\lambda f(x) - \lambda g(y_q)} \prod_{j \neq q} \int_{-\infty}^{\infty} G_t(x'|y_j) e^{\lambda f(x') - \lambda g(y_j)} dx'. \end{aligned} \quad (\text{S6})$$

The higher order correlations with the density are also accessible in the same way, for instance,

$$\begin{aligned} \langle \rho(x,t) \rho(y,t) e^{\lambda \mathcal{O}_t} \rangle &= \sum_{n,m} \int_{-\infty}^{\infty} dx_1 \cdots dx_N \delta(x - x_n) \delta(y - x_m) K_t(\{x_i\}|\{y_i\}) \prod_{i=1}^N e^{\lambda(f(x_i) - g(y_i))} \\ &= \frac{1}{N!} \sum_{n \neq m} \sum_{\sigma} \tilde{G}_t(x|y_{\sigma(n)}) \tilde{G}_t(y|y_{\sigma(m)}) \prod_{i \neq n,m} \int_{-\infty}^{\infty} \tilde{G}_t(x'|y_{\sigma(i)}) dx' \\ &\quad + \frac{1}{N!} \sum_n \sum_{\sigma} \tilde{G}_t(x|y_{\sigma(n)}) \delta(x - y) \prod_{i \neq n} \int_{-\infty}^{\infty} \tilde{G}_t(x'|y_{\sigma(i)}) dx' \\ &= \sum_{q \neq p} \tilde{G}_t(x|y_q) \tilde{G}_t(y|y_p) \prod_{j \neq p,q} \int_{-\infty}^{\infty} \tilde{G}_t(x'|y_j) dx' \\ &\quad + \delta(x - y) \sum_q \tilde{G}_t(x|y_q) \prod_{j \neq q} \int_{-\infty}^{\infty} \tilde{G}_t(x'|y_j) dx', \end{aligned} \quad (\text{S7})$$

where we have denoted $\tilde{G}_t(x|y) = e^{\lambda f(x)} G_t(x|y) e^{-\lambda g(y)}$. To take the average over the initial condition, we need to treat separately the annealed and quenched cases.

B. Average over the initial positions in the annealed case

In the annealed case, we compute

$$\overline{\langle e^{\lambda \mathcal{O}_t} \rangle} = \left(\frac{1}{N} \int dy \rho_0(y) e^{-\lambda g(y)} \int G_t(x|y) e^{\lambda f(x)} dx \right)^N. \quad (\text{S8})$$

For finite N , the condition $\int \rho_0 = N$ ensures that the above integrals are convergent. But in the limit $N \rightarrow \infty$ this would not be the case. Take for instance a constant density profile $\rho_0(x) = \rho$, then the integral would diverge in the domains ($x > 0, y > 0$) and ($x < 0, y < 0$). We can solve this issue by writing the above expression as

$$\overline{\langle e^{\lambda \mathcal{O}_t} \rangle} = \left(1 + \frac{1}{N} \int dy \rho_0(y) \int G_t(x|y) (e^{\lambda f(x) - \lambda g(y)} - 1) dx \right)^N, \quad (\text{S9})$$

where we have used that $\int G_t(x|y) dx = 1$. In this expression, if x and y are large, with the same sign, the integrand vanishes. And if they are both large with opposite signs, $G_t(x|y)$ is small. Therefore, the integral is always well defined, and thus

$$\psi_A(\lambda, t) \equiv \lim_{N \rightarrow \infty} \ln \overline{\langle e^{\lambda \mathcal{O}_t} \rangle} = \int dy \rho_0(y) \int G_t(x|y) (e^{\lambda f(x) - \lambda g(y)} - 1) dx. \quad (\text{S10})$$

To compute the density profiles, we need

$$\overline{\langle \rho(x, t) e^{\lambda \mathcal{O}_t} \rangle} = \left(\int dy \rho_0(y) G_t(x|y) e^{\lambda f(x) - \lambda g(y)} \right) \left(\frac{1}{N} \int dy \rho_0(y) e^{-\lambda g(y)} \int G_t(x'|y) e^{\lambda f(x')} dx' \right)^{N-1}. \quad (\text{S11})$$

Taking the ratio with (S9) and using the same rewriting as before, we get

$$\frac{\overline{\langle \rho(x, t) e^{\lambda \mathcal{O}_t} \rangle}}{\overline{\langle e^{\lambda \mathcal{O}_t} \rangle}} = \frac{e^{\lambda f(x)} \int dy \rho_0(y) G_t(x|y) e^{-\lambda g(y)}}{1 + \frac{1}{N} \int dy \rho_0(y) \int G_t(x'|y) (e^{\lambda f(x') - \lambda g(y)} - 1) dx'}. \quad (\text{S12})$$

In the limit $N \rightarrow \infty$, this becomes

$$\psi_A(x, \lambda, t) \equiv \lim_{N \rightarrow \infty} \frac{\overline{\langle \rho(x, t) e^{\lambda \mathcal{O}_t} \rangle}}{\overline{\langle e^{\lambda \mathcal{O}_t} \rangle}} = e^{\lambda f(x)} \int dy \rho_0(y) G_t(x|y) e^{-\lambda g(y)}. \quad (\text{S13})$$

For the two points correlation function, we need to compute

$$\begin{aligned} \overline{\langle \rho(x, t) \rho(y, t) e^{\lambda \mathcal{O}_t} \rangle} = & \sum_{q \neq p} \left(\int_{-\infty}^{\infty} dz \frac{\rho_0(z)}{N} \tilde{G}_t(x|z) \right) \left(\int_{-\infty}^{\infty} dz \frac{\rho_0(z)}{N} \tilde{G}_t(y|z) \right) \left(\int_{-\infty}^{\infty} dz \frac{\rho_0(z)}{N} \int_{-\infty}^{\infty} dx' \tilde{G}_t(x'|z) \right)^{N-2} \\ & + \delta(x - y) \sum_q \left(\int_{-\infty}^{\infty} dz \frac{\rho_0(z)}{N} \tilde{G}_t(x|z) \right) \left(\int_{-\infty}^{\infty} dz \frac{\rho_0(z)}{N} \int_{-\infty}^{\infty} dx' \tilde{G}_t(x'|z) \right)^{N-1}. \end{aligned} \quad (\text{S14})$$

The sums no longer depend on p and q , and thus,

$$\begin{aligned} \overline{\langle \rho(x, t) \rho(y, t) e^{\lambda \mathcal{O}_t} \rangle} = & \frac{N-1}{N} \left(\int_{-\infty}^{\infty} dz \rho_0(z) \tilde{G}_t(x|z) \right) \left(\int_{-\infty}^{\infty} dz \rho_0(z) \tilde{G}_t(y|z) \right) \left(\int_{-\infty}^{\infty} dz \frac{\rho_0(z)}{N} \int_{-\infty}^{\infty} dx' \tilde{G}_t(x'|z) \right)^{N-2} \\ & + \delta(x - y) \left(\int_{-\infty}^{\infty} dz \rho_0(z) \tilde{G}_t(x|z) \right) \left(\int_{-\infty}^{\infty} dz \frac{\rho_0(z)}{N} \int_{-\infty}^{\infty} dx' \tilde{G}_t(x'|z) \right)^{N-1}. \end{aligned} \quad (\text{S15})$$

Taking the ratio with (S9), and using again the same rewriting for the denominator, we get for $N \rightarrow \infty$,

$$\lim_{N \rightarrow \infty} \frac{\overline{\langle \rho(x, t) \rho(y, t) e^{\lambda \mathcal{O}_t} \rangle}}{\langle e^{\lambda \mathcal{O}_t} \rangle} = \delta(x - y) \left(\int_{-\infty}^{\infty} dz \rho_0(z) G_t(x|z) e^{\lambda f(x) - \lambda g(z)} \right) + \left(\int_{-\infty}^{\infty} dz \rho_0(z) G_t(x|z) e^{\lambda f(x) - \lambda g(z)} \right) \left(\int_{-\infty}^{\infty} dz \rho_0(z) G_t(y|z) e^{\lambda f(x) - \lambda g(z)} \right). \quad (\text{S16})$$

In particular, we have

$$\lim_{N \rightarrow \infty} \left[\frac{\overline{\langle \rho(x, t) \rho(y, t) e^{\lambda \mathcal{O}_t} \rangle}}{\langle e^{\lambda \mathcal{O}_t} \rangle} - \frac{\overline{\langle \rho(x, t) e^{\lambda \mathcal{O}_t} \rangle}}{\langle e^{\lambda \mathcal{O}_t} \rangle} \frac{\overline{\langle \rho(y, t) e^{\lambda \mathcal{O}_t} \rangle}}{\langle e^{\lambda \mathcal{O}_t} \rangle} \right] = \delta(x - y) w_A(x, \lambda, t). \quad (\text{S17})$$

C. Average over the initial positions in the quenched case

In the quenched case, the cumulant generating function is given by

$$\ln \langle e^{\lambda \mathcal{O}_t} \rangle = \sum_i \frac{1}{N} \int dy \rho_0(y) \ln \left[\int_{-\infty}^{\infty} G_t(x|y) e^{\lambda f(x) - \lambda g(y)} dx \right]. \quad (\text{S18})$$

The terms in the sum are independent of i , and the integral converges in the limit $N \rightarrow \infty$, thus

$$\psi_Q(\lambda, t) \equiv \lim_{N \rightarrow \infty} \overline{\ln \langle e^{\lambda \mathcal{O}_t} \rangle} = \int dy \rho_0(y) \ln \left[\int_{-\infty}^{\infty} G_t(x|y) e^{\lambda f(x) - \lambda g(y)} dx \right]. \quad (\text{S19})$$

Similarly, for the profiles we compute

$$\frac{\overline{\langle \rho(x, t) e^{\lambda \mathcal{O}_t} \rangle}}{\langle e^{\lambda \mathcal{O}_t} \rangle} = \sum_q \frac{G_t(x|y_q) e^{\lambda f(x) - \lambda g(y_q)}}{\int_{-\infty}^{\infty} G_t(x'|y_q) e^{\lambda f(x') - \lambda g(y_q)} dx'}. \quad (\text{S20})$$

We can easily take the average over the initial positions y_i , which gives

$$w_Q(x, \lambda, t) \equiv \lim_{N \rightarrow \infty} \frac{\overline{\langle \rho(x, t) e^{\lambda \mathcal{O}_t} \rangle}}{\langle e^{\lambda \mathcal{O}_t} \rangle} = \int dy \rho_0(y) \frac{G_t(x|y) e^{\lambda f(x) - \lambda g(y)}}{\int_{-\infty}^{\infty} G_t(x'|y) e^{\lambda f(x') - \lambda g(y)} dx'}. \quad (\text{S21})$$

Finally, for the two points correlation functions, we have

$$\frac{\overline{\langle \rho(x, t) \rho(y, t) e^{\lambda \mathcal{O}_t} \rangle}}{\langle e^{\lambda \mathcal{O}_t} \rangle} = \sum_{q \neq p} \frac{\tilde{G}_t(x|y_p)}{\int_{-\infty}^{\infty} \tilde{G}_t(x'|y_p) dx'} \frac{\tilde{G}_t(y|y_q)}{\int_{-\infty}^{\infty} \tilde{G}_t(x'|y_q) dx'} + \delta(x - y) \sum_q \frac{\tilde{G}_t(x|y_q)}{\int_{-\infty}^{\infty} \tilde{G}_t(x'|y_q) dx'}. \quad (\text{S22})$$

Averaging over the initial condition yields

$$\frac{\overline{\langle \rho(x, t) \rho(y, t) e^{\lambda \mathcal{O}_t} \rangle}}{\langle e^{\lambda \mathcal{O}_t} \rangle} = \delta(x - y) \int_{-\infty}^{\infty} dz \rho_0(z) \frac{\tilde{G}_t(x|z)}{\int_{-\infty}^{\infty} \tilde{G}_t(x'|z) dx'} + \frac{N-1}{N} \left(\int_{-\infty}^{\infty} dz \rho_0(z) \frac{\tilde{G}_t(x|z)}{\int_{-\infty}^{\infty} \tilde{G}_t(x'|z) dx'} \right) \left(\int_{-\infty}^{\infty} dz \rho_0(z) \frac{\tilde{G}_t(y|z)}{\int_{-\infty}^{\infty} \tilde{G}_t(x'|z) dx'} \right). \quad (\text{S23})$$

In the large N limit, this gives

$$\lim_{N \rightarrow \infty} \left[\frac{\overline{\langle \rho(x, t) \rho(y, t) e^{\lambda \mathcal{O}_t} \rangle}}{\langle e^{\lambda \mathcal{O}_t} \rangle} - \frac{\overline{\langle \rho(x, t) e^{\lambda \mathcal{O}_t} \rangle}}{\langle e^{\lambda \mathcal{O}_t} \rangle} \frac{\overline{\langle \rho(y, t) e^{\lambda \mathcal{O}_t} \rangle}}{\langle e^{\lambda \mathcal{O}_t} \rangle} \right] = \delta(x - y) w_Q(x, \lambda, t), \quad (\text{S24})$$

as in the annealed case.

D. Applications

In all the following applications, we consider an initial density of particles $\rho_0(x) = \rho_+\Theta(x) + \rho_-\Theta(-x)$ for simplicity, and consider the case of the current Q_t , corresponding to $f(x) = g(x) = \Theta(x)$.

1. Brownian particles

As a first application, we revisit the well-studied case of reflecting Brownian particles on the real line. The propagator of an individual particle with diffusion coefficient D is $G_t(x|y) = e^{-\frac{(x-y)^2}{4Dt}} / \sqrt{4\pi Dt}$. Using this propagator in the general expressions (S10,S13), we obtain $\psi_A(\lambda, t) = \omega\sqrt{\frac{Dt}{\pi}}$ and

$$w_A(x > 0, \lambda, t) = \rho_+ + \frac{\rho_- e^\lambda - \rho_+}{2} \operatorname{erfc}\left(\frac{x}{\sqrt{4Dt}}\right), \quad (\text{S25})$$

where we have denoted $\omega = \rho_+(e^{-\lambda} - 1) + \rho_-(e^\lambda - 1)$, by analogy with the single parameter identified in the simple exclusion process (SEP) [1]. Indeed, these expressions coincide with the low density limit of the ones obtained for the SEP [1–3]. The profile for $x < 0$ can be deduced from the symmetry $x \rightarrow -x$, $\lambda \rightarrow -\lambda$, $\rho_\pm \rightarrow \rho_\mp$. Similarly, in the quenched case, we recover the expression found in [4] for the cumulants, and we additionally get the correlation profiles,

$$w_Q(x, \lambda, t) = e^{\lambda\Theta(x)} \int_{-\infty}^{\infty} \rho_0(y) \frac{e^{-\left(\frac{x}{\sqrt{4Dt}} - y\right)^2}}{1 + \frac{e^\lambda - 1}{2} \operatorname{erfc}(-y)} \frac{dy}{\sqrt{\pi}}. \quad (\text{S26})$$

A related expression for constant ρ_0 can be found in [5]. The two profiles w_A and w_Q are represented in Fig. S5 (solid black lines).

2. Run and tumble particles

The Laplace transform of the propagator of an individual particle takes a simple form [6],

$$\int_0^\infty e^{-st} G_t(x|y) dt = \frac{\Lambda(s)}{2s} e^{-\Lambda(s)|x-y|}, \quad (\text{S27})$$

where $\Lambda(s) = \sqrt{s(s+2\gamma)}/v_0$. We can easily obtain the annealed profile and cumulant generating function in the Laplace domain since the expressions (S10,S13) are linear in the propagator. The inverse Laplace transform can be computed explicitly using the expressions given in [7], and we get $\psi_A(\lambda, t) = \frac{\omega}{2} v_0 t e^{-\gamma t} (\mathbf{I}_0(\gamma t) + \mathbf{I}_1(\gamma t))$, where we have again denoted $\omega = \rho_+(e^{-\lambda} - 1) + \rho_-(e^\lambda - 1)$, by analogy with the single parameter identified in the simple exclusion process (SEP) [1], and \mathbf{I}_ν is a modified Bessel function. Similarly, the correlation profile reads

$$w_A(x > 0, \lambda, t) = \rho_+ + \frac{\rho_- e^\lambda - \rho_+}{2} \Theta(v_0 t - x) \left(e^{-\frac{\gamma x}{v_0}} + \frac{\gamma x}{v_0} \int_1^{\frac{v_0 t}{x}} \frac{e^{-\frac{\gamma x T}{v_0}} \mathbf{I}_1\left(\frac{\gamma x}{v_0} \sqrt{T^2 - 1}\right)}{\sqrt{T^2 - 1}} dT \right). \quad (\text{S28})$$

The expression for $x < 0$ can again be obtained by symmetry. Finally, in the large time limit, ψ_A and w_A (S28) reduce to the Brownian case, with a diffusion coefficient $D = v_0^2/(2\gamma)$.

3. Lévy flights

Next, as an illustration of non diffusive dynamics at long times, we consider particles performing Lévy flights, corresponding to an individual propagator

$$G_t(x|y) = \frac{1}{t^{1/\alpha}} g\left(\frac{x-y}{t^{1/\alpha}}\right), \quad g(x) = \int_{-\infty}^{\infty} e^{-ikx - |k|^\alpha} \frac{dk}{2\pi}, \quad (\text{S29})$$

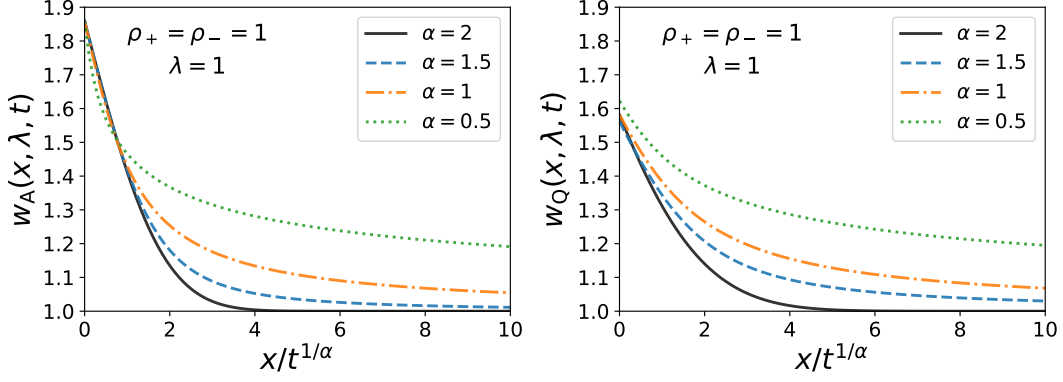


FIG. S5. Annealed correlation profile w_A (left) and quenched correlation profile w_Q (right) for Lévy particles, for different values of the Lévy exponent α . They are compared to the one of the Brownian particles with $D = 1$, corresponding to $\alpha = 2$ (black solid line). For $0 < \alpha < 2$, the correlation profiles decay as a power law, as $x^{-\alpha}$, while for the Brownian particles, the decay is much faster, as $e^{-\frac{x^2}{4Dt}}/x$.

with the exponent $\alpha \in [0, 2]$. Plugging this expression into the formulas (S13) for w_A and (S21) for w_Q , we obtain that these two profiles are functions of $x/t^{1/\alpha}$ only. The annealed profile reads

$$w_A(x = zt^{1/\alpha}, \lambda, t) = \rho_+ + (\rho_- e^\lambda - \rho_+) \int_z^\infty g(y) dy, \quad (\text{S30})$$

for $x > 0$. Similarly, the quenched profile is

$$w_Q(x = zt^{1/\alpha}, \lambda, t) = e^{\lambda\Theta(z)} \left[\rho_+ \int_0^\infty dy \frac{g(z-y)}{1 + (e^\lambda - 1) \int_{-y}^\infty g(u) du} + \rho_- \int_{-\infty}^0 dy \frac{g(z-y)}{1 + (e^\lambda - 1) \int_{-y}^\infty g(u) du} \right]. \quad (\text{S31})$$

They are represented for different values of α in Fig. S5. The correlations present a power law behaviour, $w_A(x, \lambda, t) - \rho_+ \underset{x \rightarrow \infty}{\sim} x^{-\alpha}$ for $0 < \alpha < 2$, due to the fact that the particles can perform large jumps in this case.

III. THE COMB GEOMETRY

A. Propagator in the continuous limit

The comb lattice is a two dimensional lattice in which all the links parallel to the x -axis have been removed, except those on the axis itself, called the backbone. The propagator $P_t(\vec{r}|\vec{s})$ of a particle performing a random walk in discrete time on this lattice is given in [8]. Its expressions depends is different if the arrival point $\vec{r} = (r_x, r_y)$ and the starting point $\vec{s} = (r'_x, r'_y)$ are on the same teeth of the comb ($r_x = r'_x$ and $r_y r'_y > 0$) or not. The (discrete) Laplace transform of the propagator reads [8]

$$\hat{P}_\xi(\vec{r}|\vec{s}) \equiv \sum_{t=0}^\infty \xi^t P_t(\vec{r}|\vec{s}) = \frac{1 + \delta_{r_y, 0}}{2} G_2(\xi) f_2(\xi)^{|r_x - r'_x|} f_1(\xi)^{|r_y| + |r'_y|}, \quad \text{if } r_x \neq r'_x \text{ or } r_y r'_y < 0, \quad (\text{S32})$$

$$\hat{P}_\xi(\vec{r}|\vec{s}) = f_1(\xi)^{|r_y - r'_y|} \left\{ \frac{1}{2} G_2(\xi) f_1(\xi)^{2\tilde{r}} + \frac{2}{\xi} f_1(\xi)^{2\tilde{r}-1} + G_1(\xi) \left[1 - f_1(\xi)^{2(\tilde{r}-1)} \right] \right\}, \quad \text{if } r_x = r'_x \text{ and } r_y r'_y > 0, \quad (\text{S33})$$

where $\tilde{r} = \min(|r_y|, |r'_y|)$, and

$$f_1(\xi) = \frac{1 - \sqrt{1 - \xi^2}}{\xi}, \quad f_2(\xi) = \frac{1 + \sqrt{1 - \xi^2} - \sqrt{2} \sqrt{1 - \xi^2 + \sqrt{1 - \xi^2}}}{\xi}, \quad (\text{S34})$$

$$G_1(\xi) = \frac{1}{\sqrt{1-\xi^2}}, \quad G_2(\xi) = \sqrt{\frac{2}{1-\xi^2 + \sqrt{1-\xi^2}}}. \quad (\text{S35})$$

One can define a continuous version of this random walk in different ways. A convenient one is to define it as the long time limit of the discrete one. We introduce a scaling parameter T and appropriately rescale space and time with T and let $T \rightarrow \infty$. We obtain a nontrivial limit with the following scalings,

$$r_x = x T^{1/4}, \quad r_y = y \sqrt{T}, \quad t = \tau T, \quad (\text{S36})$$

with x , y and τ fixed. This implies $t \rightarrow \infty$ when $T \rightarrow \infty$, corresponding to $\xi \rightarrow 1$, such that $1 - \xi = u/T$ in the Laplace domain. Inserting these scaling into the propagator (S32), we get,

$$\hat{P}_\xi(\vec{r}|\vec{r}') \underset{T \rightarrow \infty}{\simeq} \frac{1}{2} \left(\frac{2T}{u} \right)^{1/4} (1 - 2^{3/4} u^{1/4} T^{-1/4})^{|x-x'| T^{1/4}} (1 - \sqrt{2u}/\sqrt{T})^{(|y|+|y'|)\sqrt{T}}. \quad (\text{S37})$$

We can define the propagator in the continuous limit as

$$\tilde{P}_u(x, y|x', y') \equiv \lim_{T \rightarrow \infty} T^{-1/4} \hat{P}_\xi(\vec{r}|\vec{r}') = \frac{1}{2} \left(\frac{2}{u} \right)^{1/4} e^{-2^{3/4} u^{1/4} |x-x'| - \sqrt{2u}(|y|+|y'|)}, \quad (\text{S38})$$

where the prefactor $T^{-1/4} = T^{1/4} \times \sqrt{T} \times (T)^{-1}$ comes from the rescaling of both space directions and time (and thus ξ). This expression holds for different teeth of the comb, thus $x \neq x'$. Taking the continuous limit of (S33) for the case of $x = x'$ (same teeth), we get

$$\tilde{P}_u(x, y|x' = x, y') \equiv \lim_{T \rightarrow \infty} T^{-1/2} \hat{P}_\xi(\vec{r}|\vec{r}') = \frac{1}{\sqrt{2u}} e^{-\sqrt{2u}|y-y'|} (1 - e^{-2\sqrt{2u} \min(|y|, |y'|)}), \quad (\text{S39})$$

where this time the prefactor $T^{-1/2} = \sqrt{T} \times (T)^{-1}$ comes from the rescaling of y and t (and not x since it is fixed). We can combine these two expression into

$$\tilde{P}_u(x, y|x', y') = \frac{1}{2^{3/4} u^{1/4}} e^{-2^{3/4} u^{1/4} |x-x'| - \sqrt{2u}(|y|+|y'|)} + \frac{1}{\sqrt{2u}} \left(e^{-\sqrt{2u}|y-y'|} - e^{-\sqrt{2u}|y+y'|} \right) \delta(x-x') \Theta(y y'), \quad (\text{S40})$$

where Θ is the Heaviside step function. Note that the second term is the Laplace transform of a propagator of a random walk on y with reflecting boundary condition at the origin. One can check that this propagator is indeed normalised by integrating over x and y ,

$$\int_{-\infty}^{\infty} dx \int_{-\infty}^{\infty} dy \tilde{P}_u(x, y|x', y') = \frac{1}{u}, \quad (\text{S41})$$

which is indeed the Laplace transform of 1.

B. Current through the bond $(0, 0) - (1, 0)$

As in the 1D case, the current through the horizontal bond $(0, 0) - (1, 0)$ can be expressed in terms of the number of particles on the right half space (this is true because the lattice is a tree). In the continuous limit, Q_t is thus again given by (S1), with $f(x) = g(x) = \Theta(x)$ as in the main text. The derivation of Section II can be straightforwardly adapted to the case of the comb by replacing the 1D integrals by two-dimensional integrals. For instance, the annealed correlation profile reads

$$w_A(x, y, \lambda, \tau) = e^{\lambda \Theta(x)} \int dx' \int dy' \rho_0(x', y') P_\tau(x, y|x', y') e^{-\lambda \Theta(x')}. \quad (\text{S42})$$

Since this expression is linear in the propagator, one can take its Laplace transform in time,

$$\tilde{w}_A(x, y, \lambda, u) \equiv \int_0^\infty w_A(x, y, \lambda, \tau) e^{-u\tau} d\tau = e^{\lambda \Theta(x)} \int dx' \int dy' \rho_0(x', y') \tilde{P}_u(x, y|x', y') e^{-\lambda \Theta(x')}. \quad (\text{S43})$$

Computing these integrals with the propagator (S40), with a constant density $\rho_0(x, y) = \rho$, we obtain,

$$\tilde{w}_A(x, y, \lambda, u) = \frac{\rho}{u} \left(1 + \frac{e^{\lambda \text{sign}(x)} - 1}{2} e^{-2^{3/4} u^{1/4} |x| - \sqrt{2u}|y|} \right). \quad (\text{S44})$$

This expression can be inverted to the time domain numerically, and is plotted in the main text. The fact that \tilde{w}_A is a function of $u^{1/4}x$ and \sqrt{uy} in the Laplace domain implies that w_A is a function of $x/\tau^{1/4}$ and $y/\sqrt{\tau}$ in the time domain.

IV. DERIVATION OF THE CUMULANTS AND CORRELATIONS FOR THE TRACER

A. Averaging over the time evolution

We consider that we have initially $2N + 1$ particles, at positions y_n , $n \in [-N, N]$. We take the middle particle to be the tracer, initially at position $y_0 = 0$. Therefore, $y_{-n} < 0$ for $n > 0$ and $y_n > 0$ for $n > 0$. The distribution $P_t(X|\{y_i\})$ of the tracer at time t is obtained by imposing that N particles remain on the left of the tracer, and N on the right,

$$P_t(X|\{y_i\}) \equiv \langle \delta(X - x_0(t)) \rangle = (2N + 1) \binom{2N}{N} \prod_{n=1}^N \int_{-\infty}^X dx_{-n} \int_X^{\infty} dx_n K_t(\{x_i\}|\{y_i\}), \quad (\text{S45})$$

where K_t is now the propagator of the $2N + 1$ particles, and we set $x_0 = X$. The combinatorial factor comes from the fact that the tracer can be any of the $(2N+1)$ particles, and then we choose N particles among the remaining $2N$ to be on the left of X . This gives,

$$P_t(x|\{y_i\}) = \frac{1}{(N!)^2} \sum_{\sigma} G_t(X|y_{\sigma(0)}) \prod_{n=1}^N \left(\int_{-\infty}^X dz G_t(z|y_{\sigma(-n)}) \right) \left(\int_X^{\infty} dz G_t(z|y_{\sigma(n)}) \right) \quad (\text{S46})$$

$$= \frac{1}{(N!)^2} \sum_{\sigma} G_t(X|y_{\sigma(0)}) \prod_{n=1}^N \left(\int_{-X}^{\infty} dz G_t(-z|y_{\sigma(-n)}) \right) \left(\int_X^{\infty} dz G_t(z|y_{\sigma(n)}) \right). \quad (\text{S47})$$

Partitioning the summations over the value of $\sigma(0)$, we get,

$$P_t(X|\{y_i\}) = \frac{1}{(N!)^2} \sum_{q=-N}^N \sum_{\sigma, \sigma(0)=q} G_t(X|y_q) \prod_{n=1}^N \left(\int_0^{\infty} dz G_t(-z|y_{\sigma(-n)} - X) \right) \left(\int_0^{\infty} dz G_t(z|y_{\sigma(n)} - X) \right). \quad (\text{S48})$$

In the product, all the terms are present, except y_q . The signs of z and n are distributed so that there are N positive and N negative ones (representing the particles on the right and on the left of the tracer respectively). Introducing $\varepsilon_n = \pm 1$ to represent these sign variables, we obtain

$$P_t(X|\{y_i\}) = \sum_{n=-N}^N G_t(X|y_n) \sum_{\varepsilon_j = \pm 1} \delta_{\sum_{j \neq n} \varepsilon_j, 0} \prod_{i \neq n} \int_0^{\infty} G_t(\varepsilon_i z | y_i - X) dz. \quad (\text{S49})$$

with the Kroenecker δ enforcing that there are N minus signs, and N plus signs. The $(N!)^2$ term cancelled with the fact that (S48) is invariant under the permutation of the N particles on the left and the N particles on the right. Representing the Kroenecker δ as

$$\delta_{x,y} = \frac{1}{2\pi} \int_{-\pi}^{\pi} d\theta e^{i(x-y)\theta}, \quad (\text{S50})$$

we get

$$P_t(X|\{y_i\}) = \int_{-\pi}^{\pi} \frac{d\theta}{2\pi} \sum_{n=-N}^N G_t(X|y_n) \prod_{j \neq n} \int_0^{\infty} (e^{i\theta} G_t(z|y_i - X) + e^{-i\theta} G_t(-z|y_i - X)) dz. \quad (\text{S51})$$

We can proceed similarly to study the average density of particles with a tracer at position X :

$$\langle \rho(x, t) \delta(x_0 - X) \rangle = \sum_{q \neq 0} \langle \delta(x - x_q) \delta(X - x_0) \rangle = \frac{(2N + 1)!}{(N!)^2} \sum_{q \neq 0} \prod_{n=1}^N \int_{-\infty}^X dx_{-n} \int_X^{\infty} dx_n K_t(\{x_i\}|\{y_i\}) \delta(x - x_q). \quad (\text{S52})$$

Splitting the sum over $q > 0$ and $q < 0$, we get

$$\begin{aligned} \langle \rho(x, t) \delta(x_0 - X) \rangle_E = & \\ & \frac{\Theta(X - x)}{(N!)^2} \sum_{q < 0} \sum_{\sigma} G_t(X|y_{\sigma(0)}) G_t(x|y_{\sigma(q)}) \prod_{n=-N, n \neq q}^{-1} \left(\int_{-\infty}^X dz G_t(z|y_{\sigma(n)}) \right) \prod_{n=1}^N \left(\int_X^{\infty} dz G_t(z|y_{\sigma(n)}) \right) \\ & + \frac{\Theta(x - X)}{(N!)^2} \sum_{q > 0} \sum_{\sigma} G_t(X|y_{\sigma(0)}) G_t(x|y_{\sigma(q)}) \prod_{n=-N}^{-1} \left(\int_{-\infty}^X dz G_t(z|y_{\sigma(n)}) \right) \prod_{n=1, n \neq q}^N \left(\int_X^{\infty} dz G_t(z|y_{\sigma(n)}) \right). \quad (\text{S53}) \end{aligned}$$

As we did for the tracer only, we can get rid of the sum over the permutations by labelling the permuted indices $\sigma(n) = j$, and introducing auxilliary variables $\varepsilon_j = \pm 1$ to keep track of the signs which originate from the integrals to the left of X or to the right of X . This gives

$$\begin{aligned} \langle \rho(x, t) \delta(x_0 - X) \rangle = & \\ & \Theta(X - x) \sum_{n=-N}^N \sum_{p \neq n} G_t(X|y_n) G_t(x|y_p) \sum_{\{\varepsilon_j\}, \varepsilon_p = -1} \delta_{\sum_{j \neq n} \varepsilon_j, 0} \prod_{i \neq n, p} \int_0^\infty G_t(\varepsilon_i z | y_i - X) dz \\ & + \Theta(x - X) \sum_{n=-N}^N \sum_{p \neq n} G_t(X|y_n) G_t(x|y_p) \sum_{\{\varepsilon_j\}, \varepsilon_p = +1} \delta_{\sum_{j \neq n} \varepsilon_j, 0} \prod_{i \neq n, p} \int_0^\infty G_t(\varepsilon_i z | y_i - X) dz. \end{aligned} \quad (\text{S54})$$

Introducing again the integral representation of the Kroenecker delta, we obtain

$$\begin{aligned} \langle \rho(x, t) \delta(x_0 - X) \rangle = & \int_{-\pi}^{\pi} \frac{d\theta}{2\pi} (e^{-i\theta} \Theta(X - x) + e^{i\theta} \Theta(x - X)) \sum_{n=-N}^N G_t(X|y_n) \sum_{p \neq n} G_t(x|y_p) \\ & \times \prod_{j \neq n, p} \int_0^\infty (e^{i\theta} G_t(z | y_i - X) + e^{-i\theta} G_t(-z | y_i - X)) dz. \end{aligned} \quad (\text{S55})$$

We can easily check that, by integrating over x , we recover $2N$ times (S51), as it should.

B. Average over the initial positions

We now average over the initial positions of the particles. We consider that the particles are distributed according to a density ρ_0 , such that

$$\int_0^\infty \rho_0(y) dy = N, \quad \int_{-\infty}^0 \rho_0(y) dy = N. \quad (\text{S56})$$

On each side of the tracer, the particles are indistinguishable, so we write the average over the positions y_n as

$$\overline{(\dots)} = \int_{-\infty}^0 \prod_{n=1}^N \frac{\rho_0(y_{-n}) dy_{-n}}{N} \int_0^\infty \prod_{n=1}^N \frac{\rho_0(y_n) dy_n}{N} (\dots). \quad (\text{S57})$$

We can thus compute

$$\begin{aligned} \overline{P_t(X|\{y_i\})} = & \int_{-\pi}^{\pi} \frac{d\theta}{2\pi} \left\{ G_t(X, 0) \left[\int_{-\infty}^0 \frac{dy}{N} \rho_0(y) \tilde{G}_t(X, y, \theta) \right]^N \left[\int_0^\infty \frac{dy}{N} \rho_0(y) \tilde{G}_t(X, y, \theta) \right]^N \right. \\ & \sum_{n=-N}^{-1} \int_{-\infty}^0 \frac{dy_{-n}}{N} \rho_0(y_{-n}) G_t(X|y_{-n}) \left[\int_{-\infty}^0 \frac{dy}{N} \rho_0(y) \tilde{G}_t(X, y, \theta) \right]^{N-1} \tilde{G}_t(X, 0, \theta) \left[\int_0^\infty \frac{dy}{N} \rho_0(y) \tilde{G}_t(X, y, \theta) \right]^N \\ & \left. + \sum_{n=1}^N \int_0^\infty \frac{dy_n}{N} \rho_0(y_n) G_t(X|y_n) \left[\int_{-\infty}^0 \frac{dy}{N} \rho_0(y) \tilde{G}_t(X, y, \theta) \right]^N \left[\int_0^\infty \frac{dy}{N} \rho_0(y) \tilde{G}_t(X, y, \theta) \right]^{N-1} \tilde{G}_t(X, 0, \theta) \right\}, \end{aligned} \quad (\text{S58})$$

with

$$\tilde{G}_t(X, y, \theta) = \int_0^\infty (e^{i\theta} G_t(z | y - X) + e^{-i\theta} G_t(-z | y - X)) dz. \quad (\text{S59})$$

We can write this expression in a more compact form, as

$$\begin{aligned} \overline{P_t(X|\{y_i\})} = & \int_{-\pi}^{\pi} \frac{d\theta}{2\pi} \left[\int_{-\infty}^0 \frac{dy}{N} \rho_0(y) \tilde{G}_t(X, y, \theta) \right]^N \left[\int_0^\infty \frac{dy}{N} \rho_0(y) \tilde{G}_t(X, y, \theta) \right]^N \left\{ G_t(X, 0) \right. \\ & \left. + N \tilde{G}_t(X, 0, \theta) \frac{\int_{-\infty}^0 dy \rho_0(y) G_t(X|y)}{\int_{-\infty}^0 dy \rho_0(y) \tilde{G}_t(X, y, \theta)} + N \tilde{G}_t(X, 0, \theta) \frac{\int_0^\infty dy \rho_0(y) G_t(X|y)}{\int_0^\infty dy \rho_0(y) \tilde{G}_t(X, y, \theta)} \right\}. \end{aligned} \quad (\text{S60})$$

In order to take the limit $N \rightarrow \infty$, we need to ensure the convergence of the integrals. We thus rewrite

$$\int_{-\infty}^0 \frac{dy}{N} \rho_0(y) \tilde{G}_t(X, y, \theta) = e^{-i\theta} + \frac{e^{i\theta} - e^{-i\theta}}{N} \int_{-\infty}^0 dy \rho_0(y) \int_0^{\infty} dz G_t(z|y - X), \quad (\text{S61})$$

$$\int_0^{\infty} \frac{dy}{N} \rho_0(y) \tilde{G}_t(X, y, \theta) = e^{i\theta} + \frac{e^{-i\theta} - e^{i\theta}}{N} \int_0^{\infty} dy \rho_0(y) \int_0^{\infty} dz G_t(-z|y - X), \quad (\text{S62})$$

which are convergent for $N \rightarrow \infty$. We thus get,

$$\begin{aligned} \lim_{N \rightarrow \infty} \langle P_t(X|\{y_i\}) \rangle_I &= \int_{-\pi}^{\pi} \frac{d\theta}{2\pi} \left\{ G_t(X, 0) \right. \\ &\quad \left. + \tilde{G}_t(X, 0, \theta) \left[e^{i\theta} \int_{-\infty}^0 dy \rho_0(y) G_t(X|y) + e^{-i\theta} \int_0^{\infty} dy \rho_0(y) G_t(X|y) \right] \right\} \\ &\exp \left[(e^{2i\theta} - 1) \int_{-\infty}^0 dy \rho_0(y) \int_0^{\infty} dz G_t(z|y - X) + (e^{-2i\theta} - 1) \int_0^{\infty} dy \rho_0(y) \int_0^{\infty} dz G_t(-z|y - X) \right]. \quad (\text{S63}) \end{aligned}$$

Let us write this expression in a more compact form, as

$$\boxed{P_t(X) = \lim_{N \rightarrow \infty} \overline{P_t(X|\{y_i\})} = \int_{-\pi}^{\pi} \frac{d\theta}{2\pi} f_{X,t}(\theta) e^{\phi_{X,t}(\theta)},} \quad (\text{S64})$$

with

$$\phi_{X,t} = (e^{2i\theta} - 1) \int_{-\infty}^0 dy \rho_0(y) \int_0^{\infty} dz G_t(z|y - X) + (e^{-2i\theta} - 1) \int_0^{\infty} dy \rho_0(y) \int_0^{\infty} dz G_t(-z|y - X), \quad (\text{S65})$$

$$f_{X,t}(\theta) = G_t(X, 0) + \tilde{G}_t(X, 0, \theta) \left[e^{i\theta} \int_{-\infty}^0 dy \rho_0(y) G_t(X|y) + e^{-i\theta} \int_0^{\infty} dy \rho_0(y) G_t(X|y) \right]. \quad (\text{S66})$$

This coincides with the expression given in [9] for constant initial density ρ_0 . Proceeding similarly from (S55), we get

$$\begin{aligned} \overline{\langle \rho(x, t) \delta(x_0 - X) \rangle} &= \int_{-\pi}^{\pi} \frac{d\theta}{2\pi} (e^{-i\theta} \Theta(X - x) + e^{i\theta} \Theta(x - X)) \\ &\quad \times \left[\int_{-\infty}^0 \frac{dy}{N} \rho_0(y) \tilde{G}_t(X, y, \theta) \right]^N \left[\int_0^{\infty} \frac{dy}{N} \rho_0(y) \tilde{G}_t(X, y, \theta) \right]^N \\ &\quad \left\{ G_t(X, 0) \left[N \frac{\int_{-\infty}^0 dy \rho_0(y) G_t(x|y)}{\int_{-\infty}^0 dy \rho_0(y) \tilde{G}_t(X, y, \theta)} + N \frac{\int_0^{\infty} dy \rho_0(y) G_t(x|y)}{\int_0^{\infty} dy \rho_0(y) \tilde{G}_t(X, y, \theta)} \right] \right. \\ &\quad \left. + G_t(x, 0) \left[N \frac{\int_{-\infty}^0 dy \rho_0(y) G_t(X|y)}{\int_{-\infty}^0 dy \rho_0(y) \tilde{G}_t(X, y, \theta)} + N \frac{\int_0^{\infty} dy \rho_0(y) G_t(X|y)}{\int_0^{\infty} dy \rho_0(y) \tilde{G}_t(X, y, \theta)} \right] \right. \\ &\quad \left. + N \tilde{G}_t(X, 0, \theta) \frac{\int_{-\infty}^0 dy \rho_0(y) G_t(X|y)}{\int_{-\infty}^0 dy \rho_0(y) \tilde{G}_t(X, y, \theta)} \left[(N-1) \frac{\int_{-\infty}^0 dy \rho_0(y) G_t(x|y)}{\int_{-\infty}^0 dy \rho_0(y) \tilde{G}_t(X, y, \theta)} + N \frac{\int_0^{\infty} dy \rho_0(y) G_t(x|y)}{\int_0^{\infty} dy \rho_0(y) \tilde{G}_t(X, y, \theta)} \right] \right. \\ &\quad \left. + N \tilde{G}_t(X, 0, \theta) \frac{\int_0^{\infty} dy \rho_0(y) G_t(X|y)}{\int_0^{\infty} dy \rho_0(y) \tilde{G}_t(X, y, \theta)} \left[N \frac{\int_{-\infty}^0 dy \rho_0(y) G_t(x|y)}{\int_{-\infty}^0 dy \rho_0(y) \tilde{G}_t(X, y, \theta)} + (N-1) \frac{\int_0^{\infty} dy \rho_0(y) G_t(x|y)}{\int_0^{\infty} dy \rho_0(y) \tilde{G}_t(X, y, \theta)} \right] \right\}. \quad (\text{S67}) \end{aligned}$$

Using the same large N analysis as before, we get

$$\begin{aligned} \lim_{N \rightarrow \infty} \overline{\langle \rho(x, t) \delta(x_0 - X) \rangle} &= \int_{-\pi}^{\pi} \frac{d\theta}{2\pi} (e^{-i\theta} \Theta(X - x) + e^{i\theta} \Theta(x - X)) \\ &\exp \left[(e^{2i\theta} - 1) \int_{-\infty}^0 dy \rho_0(y) \int_0^{\infty} dz G_t(z|y - X) + (e^{-2i\theta} - 1) \int_0^{\infty} dy \rho_0(y) \int_0^{\infty} dz G_t(-z|y - X) \right] \\ &\left\{ \left[G_t(X, 0) + \tilde{G}_t(X, 0, \theta) \left(e^{i\theta} \int_{-\infty}^0 dy \rho_0(y) G_t(X|y) + e^{-i\theta} \int_0^{\infty} dy \rho_0(y) G_t(X|y) \right) \right] \right. \\ &\quad \times \left[e^{i\theta} \int_{-\infty}^0 dy \rho_0(y) G_t(x|y) + e^{-i\theta} \int_0^{\infty} dy \rho_0(y) G_t(x|y) \right] \\ &\quad \left. + G_t(x, 0) \left[e^{i\theta} \int_{-\infty}^0 dy \rho_0(y) G_t(X|y) + e^{-i\theta} \int_0^{\infty} dy \rho_0(y) G_t(X|y) \right] \right\}. \end{aligned} \quad (\text{S68})$$

Isolating the dependence in x , we can write the conditional profile in a compact form as

$$\boxed{\lim_{N \rightarrow \infty} \frac{\overline{\langle \rho(x, t) \delta(x_0 - X) \rangle}}{\overline{\langle \delta(x_0 - X) \rangle}} = \alpha_t^{\pm}(X) G_t(x|0) + \beta_t^{\pm}(X) \int_{\mathbb{R}^{\mp}} \rho_0(y) G_t(x|y) dy + \int_{\mathbb{R}^{\pm}} \rho_0(y) G_t(x|y) dy,} \quad (\text{S69})$$

with the \pm signs corresponding to $x \gtrless X$

$$\alpha_t^{\pm}(X) = \frac{\int_{-\pi}^{\pi} d\theta e^{\pm i\theta} g_{X,t}(\theta) e^{\phi_{X,t}(\theta)}}{\int_{-\pi}^{\pi} d\theta f_{X,t}(\theta) e^{\phi_{X,t}(\theta)}}, \quad \beta_t^{\pm}(X) = \frac{\int_{-\pi}^{\pi} d\theta e^{\pm 2i\theta} f_{X,t}(\theta) e^{\phi_{X,t}(\theta)}}{\int_{-\pi}^{\pi} d\theta f_{X,t}(\theta) e^{\phi_{X,t}(\theta)}}, \quad (\text{S70})$$

with

$$g_{X,t}(\theta) = e^{i\theta} \int_{-\infty}^0 dy \rho_0(y) G_t(X|y) + e^{-i\theta} \int_0^{\infty} dy \rho_0(y) G_t(X|y). \quad (\text{S71})$$

For a step initial density profile, G_t invariant by translation and symmetric, these expressions reduce to the ones given in the main text.

V. THE CASE OF TWO TRACERS

Let us consider the joint distribution of the positions of two tracers, denoted $x_0(t)$ and $x_K(t)$, with $x_0(t) < x_K(t)$ without loss of generality. We assume that there are initially $K - 1$ particles between the two tracers, at positions $x_n(t)$, $1 \leq n < K$. Initially, we have $x_0(0) = 0$, and $x_K(0) = Y_0$. As in the previous case, we place N particles on the left of x_0 , denoted x_{-n} for $0 < n \leq N$, and N particles on the right of x_K , denoted x_n with $K < n \leq N + K$. We consider that these particles are initially distributed according to a density ρ_0 such that

$$\int_{-\infty}^0 \rho_0 = N, \quad \int_0^{Y_0} \rho_0 = K - 1, \quad \int_{Y_0}^{\infty} \rho_0 = N. \quad (\text{S72})$$

We will compute the averages over the time evolution of the particles, and their initial positions for finite N , and then let $N \rightarrow \infty$.

A. Averaging over the time evolution

The computations are similar to the case of one tracer, except that we must now enforce two constraints: the number N of particles on the left of x_0 is fixed, and the number N of particles to the right of x_K is also fixed. The total number of particles being conserved by the joint propagator, this automatically enforces that there are $K - 1$ particles between x_0 and x_K . We again denote $\{y_i\}$ the initial positions of the particles. We get,

$$\begin{aligned} P_t(X, Y | \{y_i\}) &\equiv \langle \delta(X - x_0(t)) \delta(Y - x_K(t)) \rangle \\ &= \int_{-\pi}^{\pi} \frac{d\theta}{2\pi} e^{-iN\theta} \int_{-\pi}^{\pi} \frac{d\varphi}{2\pi} e^{-iN\varphi} \sum_{n=-N}^{N+K} G_t(X|y_n) \sum_{m \neq n} G_t(Y|y_m) \prod_{j \neq n, m} (I_L(y_j) e^{i\theta} + I_C(y_j) + I_R(y_j) e^{i\varphi}), \end{aligned} \quad (\text{S73})$$

where we have defined

$$I_L(y) = \int_{-\infty}^X G_t(z|y)dz, \quad I_C(y) = \int_X^Y G_t(z|y)dz, \quad I_R(y) = \int_Y^{\infty} G_t(z|y)dz. \quad (\text{S74})$$

The integrals over the two phases in (S73) enforce the two conservation constraints. Eq. (S73) is the analogous to Eq. (S51) obtained for one tracer. This reasoning can be extended to an arbitrary number of tracers. The same procedure can be used to obtain

$$\begin{aligned} \langle \delta(X - x_0(t))\delta(Y - x_K(t))\rho(x, t) \rangle &= \int_{-\pi}^{\pi} \frac{d\theta}{2\pi} e^{-iN\theta} \int_{-\pi}^{\pi} \frac{d\varphi}{2\pi} e^{-iN\varphi} (e^{i\theta}\Theta(X - x) + \Theta(x - X)\Theta(Y - x) + e^{i\varphi}\Theta(x - Y)) \\ &\sum_p G_t(x|y_p) \sum_{n \neq p} G_t(X|y_n) \sum_{m \neq n, p} G_t(Y|y_m) \prod_{j \neq p, n, m} (I_L(y_j)e^{i\theta} + I_C(y_j) + I_R(y_j)e^{i\varphi}). \end{aligned} \quad (\text{S75})$$

B. Averaging over the initial condition

We must now compute the average over the initial positions $\{y_i\}$, defined as

$$\overline{f(\{y_i\})} = \int_{-\infty}^0 \prod_{n=1}^N \frac{dy_{-n}}{N} \int_0^{Y_0} \prod_{n=1}^K \frac{dy_n}{K-1} \int_{Y_0}^{\infty} \prod_{n=K+1}^{K+N} \frac{dy_n}{N} f(y_{-N}, \dots, y_{-1}, 0, y_1, \dots, y_{K-1}, Y_0, y_{K+1}, \dots, y_{N+K}). \quad (\text{S76})$$

Performing this averaging for the probability (S73), we obtain,

$$\begin{aligned} P_t(X, Y) &\equiv \overline{P_t(X, Y|\{y_i\})} = \int_{-\pi}^{\pi} \frac{d\theta}{2\pi} e^{-iN\theta} \int_{-\pi}^{\pi} \frac{d\varphi}{2\pi} e^{-iN\varphi} [J_L]^N [J_C]^{K-1} [J_R]^N \left\{ G_t(X|0)G_t(Y|Y_0) + G_t(X|Y_0)G_t(Y|0) \right. \\ &+ G_t(X|0) \left[\frac{\int_{-\infty}^0 \rho_0(y)G_t(Y|y)dy}{J_L} + \frac{\int_0^{Y_0} \rho_0(y)G_t(Y|y)dy}{J_C} + \frac{\int_{Y_0}^{\infty} \rho_0(y)G_t(Y|y)dy}{J_R} \right] [I_L(Y_0)e^{i\theta} + I_C(Y_0) + I_R(Y_0)e^{i\varphi}] \\ &+ G_t(X|Y_0) \left[\frac{\int_{-\infty}^0 \rho_0(y)G_t(Y|y)dy}{J_L} + \frac{\int_0^{Y_0} \rho_0(y)G_t(Y|y)dy}{J_C} + \frac{\int_{Y_0}^{\infty} \rho_0(y)G_t(Y|y)dy}{J_R} \right] [I_L(0)e^{i\theta} + I_C(0) + I_R(0)e^{i\varphi}] \\ &+ G_t(Y|0) \left[\frac{\int_{-\infty}^0 \rho_0(y)G_t(Y|y)dy}{J_L} + \frac{\int_0^{Y_0} \rho_0(y)G_t(Y|y)dy}{J_C} + \frac{\int_{Y_0}^{\infty} \rho_0(y)G_t(Y|y)dy}{J_R} \right] [I_L(Y_0)e^{i\theta} + I_C(Y_0) + I_R(Y_0)e^{i\varphi}] \\ &+ G_t(Y|Y_0) \left[\frac{\int_{-\infty}^0 \rho_0(y)G_t(Y|y)dy}{J_L} + \frac{\int_0^{Y_0} \rho_0(y)G_t(Y|y)dy}{J_C} + \frac{\int_{Y_0}^{\infty} \rho_0(y)G_t(Y|y)dy}{J_R} \right] [I_L(0)e^{i\theta} + I_C(0) + I_R(0)e^{i\varphi}] \\ &\left. + [I_L(0)e^{i\theta} + I_C(0) + I_R(0)e^{i\varphi}] [I_L(Y_0)e^{i\theta} + I_C(Y_0) + I_R(Y_0)e^{i\varphi}] \times \left[\right. \right. \\ &\quad \frac{\int_{-\infty}^0 \rho_0(y)G_t(X|y)dy}{J_L} \left(\frac{N-1}{N} \frac{\int_{-\infty}^0 \rho_0(y)G_t(Y|y)dy}{J_L} + \frac{\int_0^{Y_0} \rho_0(y)G_t(Y|y)dy}{J_C} + \frac{\int_{Y_0}^{\infty} \rho_0(y)G_t(Y|y)dy}{J_R} \right) \\ &\quad + \frac{\int_0^{Y_0} \rho_0(y)G_t(Y|y)dy}{J_C} \left(\frac{\int_{-\infty}^0 \rho_0(y)G_t(Y|y)dy}{J_L} + \frac{K-2}{K-1} \frac{\int_0^{Y_0} \rho_0(y)G_t(Y|y)dy}{J_C} + \frac{\int_{Y_0}^{\infty} \rho_0(y)G_t(Y|y)dy}{J_R} \right) \\ &\quad \left. \left. + \frac{\int_{Y_0}^{\infty} \rho_0(y)G_t(Y|y)dy}{J_R} \left(\frac{\int_{-\infty}^0 \rho_0(y)G_t(Y|y)dy}{J_L} + \frac{\int_0^{Y_0} \rho_0(y)G_t(Y|y)dy}{J_C} + \frac{N-1}{N} \frac{\int_{Y_0}^{\infty} \rho_0(y)G_t(Y|y)dy}{J_R} \right) \right] \right\} \quad (\text{S77}) \end{aligned}$$

where

$$J_L = \int_{-\infty}^0 \frac{dy}{N} \rho_0(y) (I_L(y)e^{i\theta} + I_C(y) + I_R(y)e^{i\varphi}), \quad J_R = \int_{Y_0}^{\infty} \frac{dy}{N} \rho_0(y) (I_L(y)e^{i\theta} + I_C(y) + I_R(y)e^{i\varphi}), \quad (\text{S78})$$

$$J_C = \int_0^{Y_0} \frac{dy}{K-1} \rho_0(y) (I_L(y)e^{i\theta} + I_C(y) + I_R(y)e^{i\varphi}). \quad (\text{S79})$$

To take the thermodynamic limit $N \rightarrow \infty$, we must regularise the expressions of J_L and J_R as

$$J_L = e^{i\theta} + \int_{-\infty}^0 \frac{dy}{N} \rho_0(y) [(I_L(y) - 1)e^{i\theta} + I_C(y) + I_R(y)e^{i\varphi}] , \quad (\text{S80})$$

$$J_R = e^{i\varphi} + \int_{Y_0}^{\infty} \frac{dy}{N} \rho_0(y) [I_L(y)e^{i\theta} + I_C(y) + (I_R(y) - 1)e^{i\varphi}] . \quad (\text{S81})$$

Taking the limit $N \rightarrow \infty$ yields

$$\boxed{\lim_{N \rightarrow \infty} P_t(X, Y) = \int_{-\pi}^{\pi} \frac{d\theta}{2\pi} \int_{-\pi}^{\pi} \frac{d\varphi}{2\pi} f_t(X, Y, Y_0, \theta, \varphi) e^{\phi_t(X, Y, Y_0, \theta, \varphi)} ,} \quad (\text{S82})$$

where

$$\begin{aligned} \phi_t(X, Y, \theta, \varphi) = \int_{-\infty}^0 dy \rho_0(y) [(I_L(y) - 1) + I_C(y)e^{-i\theta} + I_R(y)e^{i(\varphi-\theta)}] \\ + \int_{Y_0}^{\infty} dy \rho_0(y) [I_L(y)e^{i(\theta-\varphi)} + I_C(y)e^{-i\varphi} + (I_R(y) - 1)] , \end{aligned} \quad (\text{S83})$$

$$\begin{aligned} f_t(X, Y, Y_0, \theta, \varphi) = [J_C]^{K-1} & \left\{ G_t(X|0)G_t(Y|Y_0) + G_t(X|Y_0)G_t(Y|0) \right. \\ & + \left(e^{-i\theta} \int_{-\infty}^0 \rho_0(y)G_t(Y|y)dy + \frac{\int_0^{Y_0} \rho_0(y)G_t(Y|y)dy}{J_C} + e^{-i\varphi} \int_{Y_0}^{\infty} \rho_0(y)G_t(Y|y)dy \right) \\ & \times \left[G_t(X|0) [I_L(Y_0)e^{i\theta} + I_C(Y_0) + I_R(Y_0)e^{i\varphi}] + G_t(X|Y_0) [I_L(0)e^{i\theta} + I_C(0) + I_R(0)e^{i\varphi}] \right. \\ & \left. + G_t(Y|0) [I_L(Y_0)e^{i\theta} + I_C(Y_0) + I_R(Y_0)e^{i\varphi}] + G_t(Y|Y_0) [I_L(0)e^{i\theta} + I_C(0) + I_R(0)e^{i\varphi}] \right] \\ & + [I_L(0)e^{i\theta} + I_C(0) + I_R(0)e^{i\varphi}] [I_L(Y_0)e^{i\theta} + I_C(Y_0) + I_R(Y_0)e^{i\varphi}] \times \left[\right. \\ & \left. \left(e^{-i\theta} \int_{-\infty}^0 \rho_0(y)G_t(Y|y)dy + \frac{\int_0^{Y_0} \rho_0(y)G_t(Y|y)dy}{J_C} + e^{-i\varphi} \int_{Y_0}^{\infty} \rho_0(y)G_t(Y|y)dy \right) \right. \\ & \left. \times \left(e^{-i\theta} \int_{-\infty}^0 \rho_0(y)G_t(X|y)dy + e^{-i\varphi} \int_{Y_0}^{\infty} \rho_0(y)G_t(Y|y)dy \right) \right. \\ & \left. + \frac{\int_0^{Y_0} \rho_0(y)G_t(Y|y)dy}{J_C} \left(e^{-i\theta} \int_{-\infty}^0 \rho_0(y)G_t(Y|y)dy + \frac{K-2}{K-1} \frac{\int_0^{Y_0} \rho_0(y)G_t(Y|y)dy}{J_C} + e^{-i\varphi} \int_{Y_0}^{\infty} \rho_0(y)G_t(Y|y)dy \right) \right] \right\} . \end{aligned} \quad (\text{S84})$$

Similarly, one can compute from (S75) the conditional profile, which takes the form

$$\begin{aligned} \lim_{N \rightarrow \infty} \frac{\overline{\langle \rho(x, t) \delta(x_0(t) - X) \delta(x_K(t) - Y) \rangle}}{\overline{\langle \delta(x_0(t) - X) \delta(x_K(t) - Y) \rangle}} = a_t^{(i)}(X, Y|Y_0)G_t(x|0) + b_t^{(i)}(X, Y|Y_0)G_t(x|Y_0) \\ + c_t^{(i)}(X, Y|Y_0) \int_{-\infty}^0 \rho_0(y)G_t(x|y)dy + d_t^{(i)}(X, Y|Y_0) \int_0^{Y_0} \rho_0(y)G_t(x|y)dy + e_t^{(i)}(X, Y|Y_0) \int_{Y_0}^{\infty} \rho_0(y)G_t(x|y)dy , \end{aligned} \quad (\text{S85})$$

where the superscripts $i = L, C, R$ respectively stand for $x < X$, $X < x < Y$, $Y < x$. The coefficients a_t , b_t , c_t , d_t and e_t are given by ratios of integrals of functions of the form (S84), which are rather cumbersome, so we do not write them explicitly here. The important point is that these coefficients do not depend on x , so that the dependence of the conditional profile in x is simply given by the propagator or its integral with the initial density.

C. Long time limit: alternative derivation

The joint distribution of the two tracers simplifies in the long time limit, if the propagator has, a scaling form

$$G_t(x|y) = \frac{1}{\sigma_t} g\left(\frac{x-y}{\sigma_t}\right), \quad (\text{S86})$$

with $\sigma_t \rightarrow \infty$ when $t \rightarrow \infty$. Let us also rescale the different parameters by σ_t ,

$$X = \xi \sigma_t, \quad Y = \xi' \sigma_t, \quad Y_0 = z \sigma_t. \quad (\text{S87})$$

One could use these scalings into (S82) and evaluate the integrals with a saddle point method. This is however quite tricky to do in practice. Instead, one could use an alternative approach, used in [10, 11] with one tracer. Here, we extend this method to two tracers. The main idea is to consider the generalised current

$$J_t(X|X_0) = \sum_n [\Theta(x_i(t) - X) - \Theta(x_i(0) - X_0)] \quad (\text{S88})$$

This observable measures the difference between the number of particles at the right of X at time t and the number of particles to the right of X_0 at $t = 0$. We define the tracer to be the first particle at the right of X_0 at $t = 0$. Its position random, but this effect will be negligible in the long time limit because of the rescaling of space (S87). Since the order of the particles is conserved, the position of the tracer at time t can be found by finding X such that $J_t(X|X_0) = 0$. The distribution of the position of the tracer is obtained, in the long time limit, by $P_t(X) = \mathbb{P}[J_t(X|X_0) = 0]$ [10, 11].

In the case of two tracers, we need the joint distribution of two currents,

$$P_t(X, Y|X_0, Y_0) = \mathbb{P}[J_t(X|X_0) = 0 \text{ and } J_t(Y|Y_0) = 0]. \quad (\text{S89})$$

In the following, we will set $X_0 = 0$, and assume $Y_0 > 0$, and thus $Y > X$.

The first step is to consider the joint cumulant generating function of the two currents,

$$\psi(\lambda, \mu) \equiv \lim_{N \rightarrow \infty} \ln \overline{\langle e^{\lambda J_t(X|0) + \mu J_t(Y|Y_0)} \rangle} = \int dy \rho_0(y) \int G_t(x|y) (e^{\lambda(\Theta(x-X) - \Theta(y)) + \mu(\Theta(x-Y) - \Theta(y-Y_0))} - 1) dx, \quad (\text{S90})$$

which follows directly from (S10) with $f(x) = \lambda\Theta(x-X) + \mu\Theta(x-Y)$ and $g(x) = \lambda\Theta(x) + \mu\Theta(x-Y_0)$. Using the scaling form (S86) for the propagator, with the definitions (S87), we get, in the case of a constant density $\rho_0(x) = \rho$,

$$\begin{aligned} \psi(\lambda, \mu) = \rho \sigma_t \{ & (e^{-\lambda} - 1)[h(-\xi) - h(z - \xi)] + (e^{-\lambda - \mu} - 1)h(z - \xi) + (e^\lambda - 1)[h(\xi) - h(\xi')] \\ & + (e^{-\mu} - 1)[h(z - \xi') - h(z - \xi)] + (e^{\lambda + \mu} - 1)h(\xi') + (e^\mu - 1)[h(\xi' - z) - h(\xi')] \}, \quad (\text{S91}) \end{aligned}$$

where we have introduced the double primitive of the propagator

$$h(x) = \int_x^\infty du \int_u^\infty dv g(v). \quad (\text{S92})$$

The joint distribution of the two currents can be obtained by a double Laplace inversion (in λ and μ) of $e^{\sigma_t \psi(\lambda, \mu)}$. In the long time limit, the integration can be performed by a saddle point method, which reduces to a Legendre transform,

$$\mathbb{P}[J_t(X|0) = \sigma_t q \text{ and } J_t(Y|Y_0) = \sigma_t q'] \simeq e^{-\sigma_t \phi(q, q')}, \quad \phi(q, q') = -\psi(\lambda^*, \mu^*) + \lambda^* q + \mu^* q', \quad (\text{S93})$$

where λ^* and μ^* are given by

$$\partial_\lambda \psi(\lambda, \mu)|_{\lambda^*, \mu^*} = q, \quad \partial_\mu \psi(\lambda, \mu)|_{\lambda^*, \mu^*} = q'. \quad (\text{S94})$$

The joint distribution of the two tracers is obtained by setting $q = q' = 0$, and takes the large deviation form,

$$P_t(X, Y|0, Y_0) \simeq e^{-\sigma_t \phi(0, 0)}. \quad (\text{S95})$$

We can obtain the behaviour of the distribution near around the mean values $X = 0$ and $Y = Y_0$ by expanding λ^* and μ^* in powers of ξ and $\xi' - z$. This gives at leading order a quadratic behaviour for ϕ ,

$$\phi(0, 0) \simeq \frac{1}{2} (\xi \quad \xi' - z) \begin{pmatrix} \frac{h(0)}{2h'(0)^2} & \frac{h(0)}{2h'(z)^2} \\ \frac{h(0)}{2h'(z)^2} & \frac{h(0)}{2h'(0)^2} \end{pmatrix}^{-1} \begin{pmatrix} \xi \\ \xi' - z \end{pmatrix}. \quad (\text{S96})$$

This gives a Gaussian behaviour around the average values, with the fluctuations directly obtained from the covariance matrix,

$$\boxed{\text{Var}(X) = \text{Var}(Y) = \frac{h(0)}{2h'(0)^2}\sigma_t, \quad \text{Cov}(X, Y) = \frac{h(z)}{2h'(0)^2}\sigma_t.} \quad (\text{S97})$$

VI. CONDITIONAL PROFILES VS CORRELATION PROFILES

We have introduced two equivalent ways to quantify the statistical properties of the position $x_0(t)$ of the tracer, and its correlations with the density $\rho(x, t)$ of particles:

(i) the cumulant generating function and the correlation profile

$$\psi_A(\lambda, t) = \ln \overline{\langle e^{\lambda x_0(t)} \rangle}, \quad w_A(x, \lambda, t) = \frac{\overline{\langle \rho(x, t) e^{\lambda x_0(t)} \rangle}}{\overline{\langle e^{\lambda x_0(t)} \rangle}}, \quad (\text{S98})$$

(ii) the distribution and the conditional profile

$$P_t(X) = \overline{\langle \delta(X - x_0(t)) \rangle}, \quad \tilde{w}_A(x, X, t) = \frac{\overline{\langle \rho(x, t) \delta(X - x_0(t)) \rangle}}{\overline{\langle \delta(X - x_0(t)) \rangle}}. \quad (\text{S99})$$

The two formulations are related by Laplace transforms,

$$e^{\psi_A(\lambda, t)} = \int_{-\infty}^{\infty} e^{\lambda X} P_t(X) dX, \quad w_A(x, \lambda, t) = \frac{\int_{-\infty}^{\infty} e^{\lambda X} \tilde{w}_A(x, X, t) P_t(X) dX}{\int_{-\infty}^{\infty} e^{\lambda X} P_t(X) dX}. \quad (\text{S100})$$

The correlation profiles can therefore be obtained from the conditional profile and vice versa. We will now see that in the long time limit, this relation greatly simplifies.

We start from the scaling form of the propagator (S86), with a step initial density $\rho_0(x) = \rho_- \Theta(-x) + \rho_+ \Theta(x)$. Plugging these into the distribution (S64), we obtain that the term $\phi_{X,t}(\theta)$ in the exponential is proportional to σ_t . The integral over θ can thus be evaluated in the limit $t \rightarrow \infty$ by a saddle point method. This gives that $P_t(X)$ takes a large deviation form,

$$P_t(X) \underset{t \rightarrow \infty}{\simeq} e^{-\sigma_t \chi(\xi = X/\sigma_t)}, \quad \chi(\xi) = \left(\sqrt{\rho_+ h(-\xi)} - \sqrt{\rho_- h(\xi)} \right)^2, \quad (\text{S101})$$

where h is the double primitive of the propagator (S92). This generalises the formula given in [12] for Brownian particles, and in [9] for a flat density $\rho_+ = \rho_-$. Importantly, this large deviation form allows to also evaluate the integrals in (S100) by a saddle point, which gives,

$$\psi_A(\lambda, t) \underset{t \rightarrow \infty}{\simeq} \sigma_t [\lambda \xi^*(\lambda) - \chi(\xi^*(\lambda))], \quad \text{and} \quad w_A(x, \lambda, t) \underset{t \rightarrow \infty}{\simeq} \tilde{w}_A(x, \sigma_t \xi^*(\lambda), t) \quad \text{where} \quad \chi'(\xi^*(\lambda)) = \lambda. \quad (\text{S102})$$

In this limit, the conditional profile and the correlation profile are thus equal. But this is not the case at arbitrary time. It turns out that the correlation profiles are easier to compute for observables of the form (S1), while the conditional profiles are more directly obtained for the position of a tracer.

-
- [1] B. Derrida and A. Gerschenfeld, *J. Stat. Phys.* **136**, 1 (2009).
 - [2] A. Poncet, A. Grabsch, P. Illien, and O. Bénichou, *Phys. Rev. Lett.* **127**, 220601 (2021).
 - [3] A. Grabsch, A. Poncet, P. Rizkallah, P. Illien, and O. Bénichou, *Sci. Adv.* **8**, eabm5043 (2022).
 - [4] B. Derrida and A. Gerschenfeld, *J. Stat. Phys.* **137**, 978 (2009).
 - [5] P. L. Krapivsky, K. Mallick, and T. Sadhu, *J. Stat. Mech: Theory Exp.* **2015**, P09007 (2015).
 - [6] G. H. Weiss, *Physica A* **311**, 381 (2002).
 - [7] T. Banerjee, S. N. Majumdar, A. Rosso, and G. Schehr, *Phys. Rev. E* **101**, 052101 (2020).
 - [8] P. Illien and O. Bénichou, *J. Phys. A Math. Theor.* **49**, 265001 (2016).
 - [9] C. Hegde, S. Sabhapandit, and A. Dhar, *Phys. Rev. Lett.* **113**, 120601 (2014).
 - [10] T. Imamura, K. Mallick, and T. Sasamoto, *Phys. Rev. Lett.* **118**, 160601 (2017).
 - [11] T. Imamura, K. Mallick, and T. Sasamoto, *Commun. Math. Phys.* **384**, 1409 (2021).
 - [12] T. Sadhu and B. Derrida, *J. Stat. Mech: Theory Exp.* **2015**, P09008 (2015).